

REVIEW ARTICLE

Osteon: Structure, Turnover, and Regeneration

Bei Chang, PhD, and Xiaohua Liu, PhD

Bone is composed of dense and solid cortical bone and honeycomb-like trabecular bone. Although cortical bone provides the majority of mechanical strength for a bone, there are few studies focusing on cortical bone repair or regeneration. Osteons (the Haversian system) form structural and functional units of cortical bone. In recent years, emerging evidences have shown that the osteon structure (including osteocytes, lamellae, lacunocanalicular network, and Haversian canals) plays critical roles in bone mechanics and turnover. Therefore, reconstruction of the osteon structure is crucial for cortical bone regeneration. This article provides a systematic summary of recent advances in osteons, including the structure, function, turnover, and regenerative strategies. First, the hierarchical structure of osteons is illustrated and the critical functions of osteons in bone dynamics are introduced. Next, the modeling and remodeling processes of osteons at a cellular level and the turnover of osteons in response to mechanical loading and aging are emphasized. Furthermore, several bioengineering approaches that were recently developed to recapitulate the osteon structure are highlighted.

Keywords: osteon, bone structure, basic multicellular unit, microcracks, bone regeneration

Impact Statement

This review provides a comprehensive summary of recent advances in osteons, especially the roles in bone formation, remodeling, and regeneration. Besides introducing the hierarchical structure and critical functions of osteons, we elucidate the modeling and remodeling of osteons at a cellular level. Specifically, we highlight the bioengineering approaches that were recently developed to mimic the hierarchical structure of osteons. We expect that this review will provide informative insights and attract increasing attentions in orthopedic community, shedding light on cortical bone regeneration in the future.

Introduction

BONE IS A complicated organ that supports various physiological activities and serves multiple functions like body support, movement facilitation, organ protection, mineral and fat storage, and hematopoiesis. Bone loss resulted from diseases, trauma, tumor, or aging impacts the life quality and even the survival of an individual. It was reported that bone grafting represented more than 2 million worldwide each year, making bone the second most common transplant tissue.^{1,2}

Although autologous, allogenic, and xenogenic bone grafts have been proven successful in clinical orthopedic reconstructive surgeries, they possess drawbacks such as donor site mobility, potential of immune rejection, or pathogen transfer.³ Therefore, bone tissue regeneration, which is capable of eliminating those drawbacks, has be-

come one of the most imperative research topics. The development of various bioengineering strategies has greatly promoted bone regeneration within animal models and inspired clinical bone loss remedies.⁴

Anatomically, bone is composed of dense and solid cortical bone and honeycomb-like trabecular cortical bone. Cortical bone accounts for ~80% of the total bone mass and performs the major function of bone. Moreover, natural bone acquires the mechanical strength mainly from cortical bone. The cortical bone possesses a compressive strength ranging from 100 to 230 MPa and a Young's modulus ranging from 10 to 20 GPa, while trabecular bone only reaches 2–12 MPa and 0.01–0.9 GPa, separately.⁵

Surprisingly, there are few studies aiming at cortical bone regeneration. Scaffolds used for bone regeneration are usually designed as porous and interconnected matrices that exhibit a trabecular bone-resembling morphology. As a

result, the regenerated bone from the porous scaffolds is trabecular bone, and a prolonged remodeling process is needed before it can bear a normal level of mechanical loading. It was reported that it took a patient months or even years to complete the remodeling process from the honeycomb-like trabecular bone to the compact cortical bone.⁴

Cortical bone is composed of primary bone and osteons in large animals and humans. Primary bone locates beneath the periosteal surface and displays a highly organized parallel-layered morphology. Indicated by a rapid growth process that leads to a large mass of new bone deposition on the existing bone surface,⁶ primary bone is regarded as a transient bone form that gradually transforms to osteons, a more mature type of bone. The characteristic morphology of osteons was first observed in the 17th century, and since then, many aspects of the osteons have been explored, including the structure, function, evolution, and turnover mechanism.

Osteons are the functional units of cortical bone. Osteons can be divided into primary osteons and secondary osteons. Primary osteons are adjacent to the primary bone where the blood vessels are surrounded by few circular lamellae. Secondary osteons, also known as the Haversian system, originate from primary osteons and form the main functional units of cortical bone. Typically, a secondary osteon presents a cylinder structure with multiple concentric lamellae that surround a central Haversian canal. Compared to primary osteons, secondary osteons are more mature and have the characteristic concentric structure and evident boundaries (cement lines) to separate them from interstitial bone or neighboring osteons.⁷ For small animals like rodents, cortical bone is parallelly aligned⁸ and only atypical, primary osteon-like structure can be observed.⁹

Compared to trabecular bone and primary cortical bone, osteons perform better physiological functions and dynamic changes, including load transmission, turnover, and self-remodeling. Within an osteon, osteocytes and the lacuno-canalicular network (LCN) sense and transduce mechanical stress, making the bone responsive to external stimuli. The concentric lamellae of osteons reduce bone porosity and function as a rigid shield to resist repetitive mechanical loading.¹⁰ The Haversian canal encompasses blood vessels and nerve fibers that provide nutrients and sensation to osteocytes residing within the lamellae. Moreover, the Haversian canal transports osteoclast and osteoblast progenitor cells to initiate cortical bone remodeling. Surprisingly, the significance of osteons in bone tissue engineering has not been well acknowledged.

This review provides a summary of osteons regarding the structure, function, turnover, and regeneration. First, the hierarchical structure of osteons, particularly the osteon components, including osteocytes, LCN, lamellae, and Haversian canal, are illustrated. In the meantime, the critical functions of osteons in bone dynamics are emphasized. Next, the modeling and remodeling of osteons at a cellular level and the turnover of osteons in response to mechanical loading and aging are summarized. Last, the bioengineering techniques that were recently developed to mimic the osteon structure are highlighted.

Methods

We thoroughly searched the literatures related to osteon with the aim to provide an overview of osteon structure,

turnover, and regeneration. The study methodology conforms to the Preferred Reporting Items for Systematic Reviews and Meta-Analyses Statement (PRISMA) for systematic reviews. All articles were searched in the database PubMed with key words “osteon,” “Haversian system,” “osteocyte,” “osteocyte lacunae,” “osteocyte canaliculi/canalicular,” “bone lamella/lamellae,” “Haversian canal,” “microcracks,” and “osteon-like.” Inclusion criteria were articles published in English before November 2020 describing the structure, turnover, and regeneration of osteons. Exclusion criteria were articles describing the application of osteon structure in anthropology and articles that failed to provide details. All abstracts of the articles selected were read, and articles of potential interest were reviewed in detail by the authors to decide inclusion or exclusion from this review. Given the heterogeneity of the characteristics studied in the included articles, a meta-analysis was not performed (Fig. 1).

Osteon Structure

A secondary osteon has a hierarchical structure that possesses unique features at three levels. First, an osteon is composed of collagen fibrils that form the nanofibrous extracellular matrix (ECM) and apatite crystals that deposit as mineral lamellae parallel to or around the collagen fibrils.¹¹ Second, the spatial structure of an osteon includes a central Haversian canal, concentric bone lamellae, orderly aligned osteocytes within the lamellae, and the LCN that accommodates the cell bodies and dendrites of osteocytes. These components form the featured morphology of an osteon and determine its critical role in bone. While the gross morphology of a typical secondary osteon is circular (type I osteons), other shapes are also observed, including type II osteons, drifting osteons,¹² and double zonal osteons.¹³ Each morphology type represents a different physiological indication that has been widely used to distinguish species, estimate ages, and assist in various anthropological studies.

The four components of osteons (osteocytes, LCN, lamellae, and Haversian canals) set the foundation of the function of osteons and are introduced in details herein (Fig. 2).

Osteocytes

Osteocytes are terminally differentiated bone cells that reside within the mineralized bone matrix. As the most common cell type in bone and accounting for over 90% of all bone cells, osteocytes are stellate-shaped cells with a number of dendrites extending from the cell body. Osteocytes lined up orderly within osteon lamellae and the longitudinal cell axes are parallel to the lamellae in which they reside. The distribution of osteocytes within an osteon is not uniform and the density of the osteocyte areal close to the cement line is the highest. As the distance from the cement line increases, the osteocyte density decreases and a three-fold decline has been observed between the cement line and the Haversian canal.¹⁴

Each osteocyte has 50–100 dendrites through which the cell communicates with neighboring osteocytes within or across the lamella to form a complex signaling network. Osteocyte dendrites even penetrate the cement line and

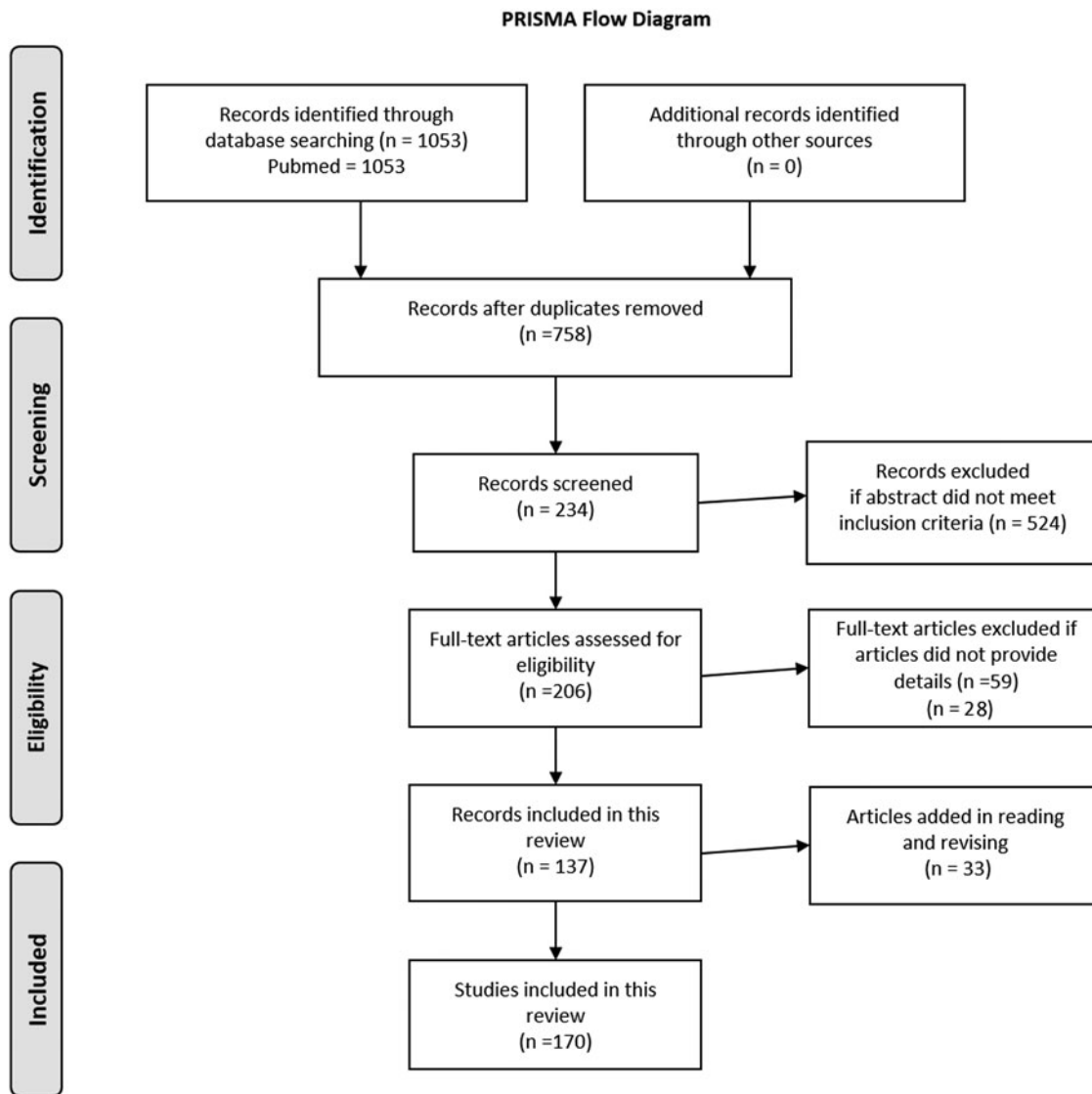


FIG. 1. The PRISMA flow diagram.

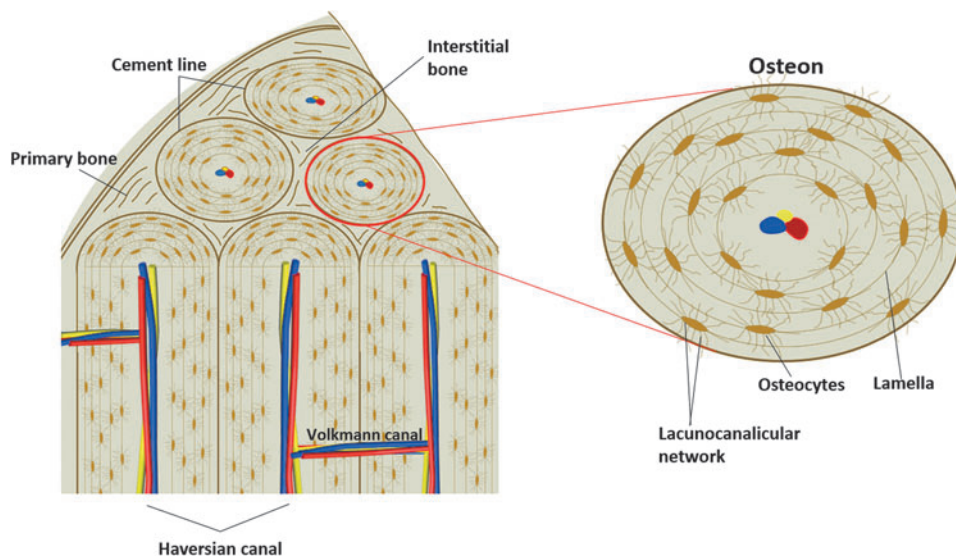


FIG. 2. Illustration of osteons, showing the spatial organization of primary bone, interstitial bone, and osteons within cortical bone (*left*), and the four components of a mature secondary osteon, including osteocytes, lacunocanalicular network, lamellae, and Haversian canal (*right*).

anchor to the surrounding interstitial bone, establishing communications between osteons and interstitial bone matrices.¹⁵ In terms of dendrite distribution, osteocytes with the plasma membrane facing bone surface (vascular membrane) have the highest number of dendrites (vascular dendrites).¹⁶ All three cytoskeletal elements (microfilaments, microtubules, and intermediate filaments) have been found in osteocyte dendrites. Microfilaments extend into the whole length of dendrites and their branches, while microtubules and intermediate filaments cease at the proximal regions of the dendrites.¹⁷ The integrity of the cytoskeleton network is a prerequisite to the shape of osteocytes and interruption of any cytoskeletal element diminishes osteocyte dendrite formation. The formation of osteocyte dendrites is also regulated by E11 protein that is specifically expressed on the cell body and dendrites of embedding osteoid osteocytes. E11 controls the number and length of osteocyte dendrites, and the conditional gene knockout of the E11/g38 decreases the number of osteon canaliculi. Moreover, the expression level of E11 is regulated by mechanical strains. Conversely, E11 is responsible for dendrite elongation in response to mechanical strains both *in vivo* and *in vitro*.¹⁸

It has been widely acknowledged that osteocytes are a group of multifunctional cells that dominate many physiological and pathological processes of bone rather than quiescent cells that are silently embedded in the bone matrix. First, osteocytes are the key regulator of bone turnover.^{19,20} Osteocytes regulate osteoclast-mediated bone absorption by modulating the RANKL/OPG expression pattern on the plasma membrane and osteoblast-mediated bone formation by releasing DKK-1 and sclerostin, two critical inhibitors of the Wnt/ β -catenin pathway. Osteocyte apoptosis caused by microcracks promotes osteoclast recruitment and activation by secreting RANKL and releasing inflammatory factors like TNF- α and interleukins.^{21,22} Besides, osteocytes have the capacity to remodel the perilacunar bone matrix directly through osteocytic osteolysis. During this process, they release Ca²⁺ and vATPase to mediate local acidification and bone matrix demineralization and other enzymes (e.g., MMP13, TRAP, and CtsK) to mediate bone proteolytic degradation.²³ Moreover, osteocytes can indirectly participate in bone turnover by secreting bioactive molecules, such as prostanoids, nitric oxide, IGF, VEGF, and TGF- β , to assist the PTH-regulated bone remodeling process. Second, osteocytes play critical roles in mechanosensation that is likely to be achieved by sensing the bone fluid flow shear stress within the LCN. The detailed mechanism of osteocyte sensation remains controversial,²⁴ but various sites of an osteocyte, including its dendrites, cell body, primary cilia,²⁵ and cell membrane receptor integrins,²⁶ have been proposed to be responsible for the sensation. Molecules such as nitric oxide, ATP, and prostaglandin have been proposed as signal mediators in this process. Third, osteocytes have endocrine functions and communicate with kidney by secreting FGF23 that regulates serum phosphorus levels. Osteocytes also participate in glucose metabolism and fertility by secreting osteocalcin.²⁷ Fourth, osteocytes are involved in inflammation²⁸ and immune regulation²⁹ by expressing RANKL/OPG on cell membrane and releasing inflammatory cytokines. Fifth, osteocytes participate in energy metabolism by regulating PPAR γ expression³⁰ and fat metabolism possibly through the central nervous system.³¹

Lacunocanalicular network

The space accommodating osteocyte cell bodies (lacunae) and osteocyte dendrites (canaliculi) within the bone matrix forms a complicated network called the LCN. The LCN has an enormous surface area that is ~ 400 times of the combination of Haversian and Volkmann canals. The high surface area of the LCN ensures osteocytes to quickly sense exterior mechanical stress and communicate with neighboring osteocytes and/or osteoblasts. Within the lacunocanalicular space, osteocytes and their dendrites do not directly contact surrounding bone matrix, instead, a thin layer of nonmineralized tissue exists between them.³² Thus, osteocytes are able to slightly move within their lacunae and osteocyte morphologies are not necessarily identical to lacuna morphologies.³³ Moreover, bone fluid flow has also been detected within the LCN when mechanical loads are applied. The fluid flow greatly facilitates osteocyte functions, including nutrient and waste product transportation, cellular behavior modulation through signaling molecule exchange, and shear stress generation for mechanosensation. Meanwhile, osteocyte viability is required for LCN remodeling in response to mechanical stress³⁴ and space maintenance by preventing pericellular mineralization.³⁵

Even though the LCN system has been observed for decades, exploration of this intricate network has just progressed in recent years owing to the advancement of bioimaging and computational modeling techniques.³⁶ For example, previous efforts to examine the changes of the LCN (e.g., the density, distribution, volume, diameter, shape, and lacuna orientation) in response to external stimuli obtained contradictory results because of the differences in examination methods or sample selections. With the advancement of the 3D imaging technology, the LCN parameters can be re-examined in a much more accurate way.³⁷ Moreover, a novel morphological feature of the LCN called canalicular junction was recently identified and characterized.³⁸ The canalicular junctions are randomly distributed within the LCN with a density similar to that of osteocyte lacunae. Even though the mechanism underlying the canalicular junction formation remains unclear, detailed observations have disputed the assumption that they were just smaller lacunae. Instead, it has been proposed that the canalicular junction greatly facilitated liquid mass transport and bone fluid flow, and therefore may have critical effects on the mechanosensation and mechanotransduction of osteocytes.

Lamellae

The concentric lamellae are the most distinguishable feature of osteons. A mature secondary osteon typically has 4–8 layers of lamellae. Under polarized light microscopy, the lamellae display alternating appearances. Lamellae parameters, including thickness,³⁹ collagen orientation,^{8,40} composition^{41,42} and mineralization level,⁴³ have been proposed as the reasons leading to the morphological and mechanical differences between the alternating lamellae. Currently, there are two theories that emphasize either the alternating tissue composition or the alternating fiber orientation is the causative factor.⁴⁴ While both theories receive increasing supports with the advancement in technology, no consensus has been reached since the approaches utilized in different studies are not comparable.

Cement lines, also known as reversal lines or resorption lines, underline the exterior boundaries of osteons. These lines are the characteristic features to distinguish primary osteons from secondary osteons, and have been described as thin lines of discontinuity formed by the activity of a basic multicellular unit (BMU) on resorbed bone surfaces. A cement line has a thickness of about 1–5 μm . The composition of the cement line has been debated for decades. Previous studies reported a remarkably higher sulfur, but lower calcium and phosphorus contents in a cement line than the surrounding bone matrix.⁴⁵ However, more recent studies showed that these are indeed hypermineralized regions with low collagen content.⁴⁶ Moreover, the level of mineralization of the cement line was positively correlated to the level of osteon mineralization. In addition, the difference in mineralization level between the cement lines and osteon lamellae decreased with the increase of osteon mineralization, indicating that the cement line mineralization is dependent on osteon mineralization and is regulated by aging. In contrast, the geometry of an osteon, including the distance of a cement line from its central Haversian canal and the diameter of the Haversian canal, did not influence the level of cement line mineralization.⁴⁷ Cement lines form the interface between interstitial bone and osteons. It was reported that the interfacial strength of cement lines was significantly lower than the shear strength of osteon lamellae; thus, debonding is more easy to occur at the cement line.⁴⁸ Besides, the mechanical strength of a cement line is different from that of interstitial bone and osteon lamellae. However, studies exploring the indentation modulus of cement lines have reported opposite results; thus, the actual mechanical strength of cement lines remains ambiguous.^{49,50}

Cement lines have been demonstrated to be an important structure influencing microcrack propagation of bone owing to the high mineralization level, distinct mechanical strength, and specific interfacial location. Numerous studies have shown that in cortical bone, microcracks form first in the interstitial bone area surrounding the cement line where the energy of microcracks is partially absorbed.^{51,52} While the fate of a microcrack is mainly determined by its inherent energy, it is also influenced by the capacity of the cement line to absorb energy when the microcrack hits a cement line. Cement lines arrest short microcracks, deflect medium-length microcracks, and alleviate the deleterious effect of long microcracks. The capacity of a cement line is regulated by the difference of the toughness between the cement line and the surrounding bone matrix. Therefore, in aged bone where the mineralization level difference between the cement line and surrounding bone matrix is reduced, microcracks are more likely to penetrate cement lines and propagate for longer distances.⁴⁷

Haversian canals

Haversian canals are the cylinder space surrounded by the innermost osteon lamella layer and are parallel to the main axis of an osteon. Haversian canals contain nerve fibers and blood vessels and provide nutrients to osteocytes. One or two blood vessels are usually seen within a Haversian canal. Studies implied that most of the vessels belong to capillaries, some occasional ones belong to venules, and very few are arterioles that can be found only on the endosteal surface of a Haversian canal.⁵³ These vessels are originated from the

endosteal blood vessel network near bone marrow.⁵³ The distribution and morphological feature of Haversian canals on the endosteal and periosteal surfaces are different. The canals are wider and denser, and tend to form a complicated network on the endosteal side, while they are narrower, sparser, and less organized on the periosteal side.⁵⁴

The wall of a Haversian canal, which is also the interior surface of the innermost lamella, is lined by a layer of flat cells that are surrounded by the densely packed collagen fiber bundles.⁵⁵ The Haversian canal marks the interface where molecular exchanges between blood circulation and bone tissue occurs. The Haversian canal is also the site where osteon remodeling starts. Volkmann canals are perpendicular to the main axis of an osteon and connect to Haversian canals. Volkmann canals are roughly the same size as Haversian canals, but have fewer numbers.⁵⁶ Both the inner walls of the Haversian and Volkmann canals are the sites where BMUs originate to initiate osteon remodeling.^{57,58} During the remodeling process, osteoclasts drill space for vascular loop migration and a Haversian canal formation is initiated. As osteoblasts deposit bone matrix to refill the cavity, vascular invagination gradually diminishes and the size of the Haversian canal decreases. Therefore, the size and shape of a Haversian canal are determined by osteoclasts and osteoblasts. Moreover, the cross-sectional area and the perimeter of a Haversian canal are positively correlated to the area of an osteon and the osteocyte number within the osteon, indicating that Haversian canals are adaptive to osteocytes.⁵⁹

Osteon Turnover

Osteons are dynamic units that are responsive to external stimuli. In this part, the formation and remodeling of osteons are discussed and possible mechanisms are provided to interpret osteon dynamics. In addition, the changes of osteonal structure in response to aging are also summarized.

Osteon modeling

Osteon modeling (formation) is observed as early as 6 months after birth in human bones,⁶⁰ and it occurs throughout the entire life. Osteon formation occurs following the resorption of pre-existing primary bone or primary osteons. The evolution significance underlying such a transition has aroused heated discussions ever since the discovery of the osteon structure and many theories have been proposed.⁶¹ One popular theory states that the osteon structure is a functional adaptation of bone to bear mechanical strains.⁶² Numerous evidences support this theory. For example, the long axis of the majority of osteons is oriented along the direction of the average loading stress and the density increases with the magnitude and frequency of daily loads.⁶³ Particularly, the osteon structure is resistant to compressive forces. Within a bovine femoral cortex, the osteons are largely limited to the posterior area, where the compressive strength is significantly higher compared to that in the anterior area.⁶⁴ Moreover, various mechanical tests (tensile, compression, and bending)^{63,65,66} and mathematical models⁸ have confirmed that osteons play a critical role in preventing bone fracture. Mechanical stress accumulates within bone generates microdamage. Within cortical bone, microdamage is localized within interstitial bone or detouring around the osteons that very rarely they penetrated

the cement lines, indicating that the osteonal structure functions as a microstructural barrier effect that delays plastic deformation and bone fracture.⁶⁵ Another theory claims that osteon modeling is a reparative response to damage. Bone reparation occurs following bone resorption. In certain conditions, osteon modeling was observed in non-osteonal bone. For example, secondary osteons are rarely seen in rat bone. However, when the rat bone was exposed to fatigue loading and underwent microcrack reparation, osteon formation was observed.⁶⁷

Osteon remodeling

Osteons are dynamic bony structures and their number, structure, and activity change over time in response to external stimuli. At a cellular level, osteon turnover is achieved by a functional complex named BMU that mainly comprises osteoclasts and osteoblasts. Within a remodeling osteon, a 3D pyramid-shaped tunnel with the following structures is formed: a cutting cone of osteoclasts in the front, a resting zone in the middle, a closing cone lined by osteoblasts following behind, and a capillary loop and supporting connective tissue in the center (Fig. 3). It is noteworthy that the tunnel-like morphology represents an idealized BMU system and various BMU morphologies such as bidirectional, branched, or clustered ones are actually observed using the 3D μ CT imaging technique.

Osteon remodeling process includes several steps, including stimuli sensation and signal transduction by osteocytes, bone absorption by osteoclasts, bone formation by osteoblasts, and the entrapment of osteoblasts (osteoblast-to-osteocyte transformation). Mechanical loading is prerequisite to initiate osteon remodeling and it creates strain-variant areas with regional differences that determine the trajectory of osteon remodeling units and the orientation of to-be-formed osteons.^{68,69} Within a remodeling tunnel, stress-strain levels are low in the loading direction and high in the transverse direction, which is shown by the flow of bone fluid within the LCN system. When loading pressure is applied, the fluid is squeezed out of the bone matrix and flows into the space at the resting zone and the closing cone,

while the fluid at the tip of the cutting cone flows toward the bone matrix. A reverse trend was observed with unloading and an outflow at the cutting cone and an inflow at the closing zone were detected.⁷⁰ High strain at the transverse direction recruited osteoblasts to the tunnel wall, while osteoclasts migrated along the loading direction where the strain was relatively low⁶⁹; thus, the remodeling path was along the longitudinal axis of osteons.

Osteocytes sense the mechanical stress and send signals to activate osteoclasts and osteoblasts to initiate bone absorption and formation, respectively.²⁴ Apart from the osteocyte-mediated signal transduction, direct communication between osteoclasts and osteoblasts is also indispensable in bone remodeling. In normal conditions, osteoblast-driven bone formation follows the path of osteoclast movement and fills up the space absorbed by osteoclasts to maintain bone mass. The close relationship between osteoclasts and osteoblasts is called coupling and multiple mechanisms have been proposed to explain this process. One mechanism is that osteoclasts degrade bone matrix and release ECM-sequestered growth factors to recruit osteoprogenitor cells and promote osteoblast differentiation. Osteoclasts also recruit osteoblasts in resorption-independent ways such as direct cell-cell contact, secreting coupling proteins, and releasing extracellular vesicles. When osteoblasts arrive at the designated area, the topography of the resorption pits directs the working path.^{71,72} Osteoclasts and pre-osteoblasts co-exist in the resting zone, and as they approach the closing zone, the pre-osteoblast density gradually increases and osteogenesis begins. When the density of the pre-osteoblasts reaches a threshold, bone formation starts and bone resorption stops. Moreover, the length of the resting zone is dependent on how fast the threshold is reached, and slower osteoblast recruitment implies more bone degradation.⁷³

The osteoblast-to-osteocyte transformation indicates the maturation of osteonal bone. With the deposit of bone matrix, osteoblasts are encased and gradually transform into osteocytes. During this process, the cell body is flattened, the cell volume is reduced, dendrites are formed, the organelle number decreases, and the nuclear-to-cytoplasm ratio increases. Once the mineralization is initiated, the number

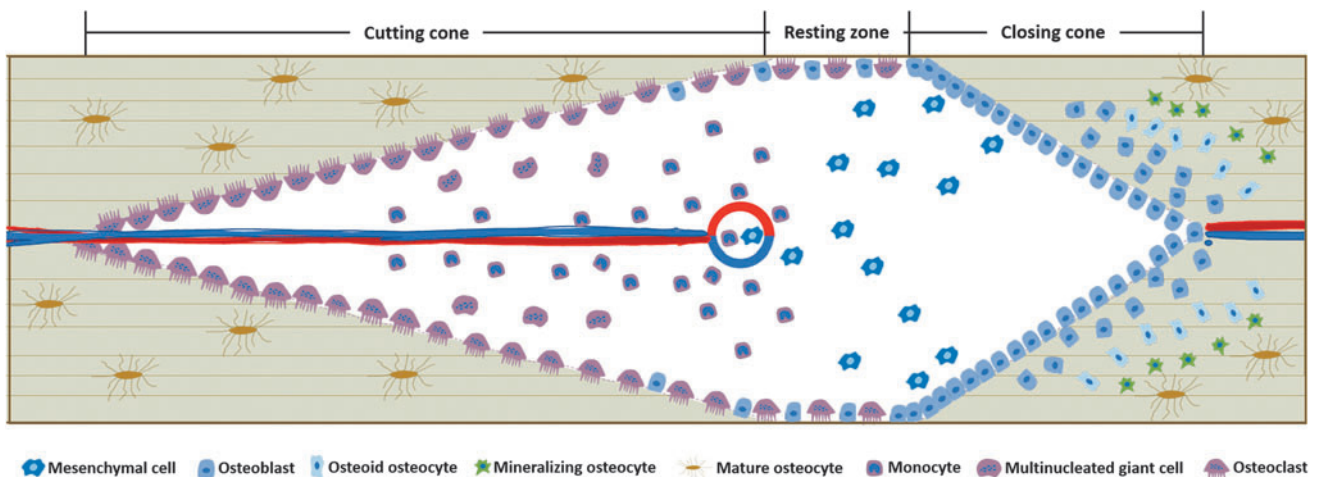


FIG. 3. Illustration of a basic BMU in osteon remodeling. Three zones are shown, including cutting cone dominated by osteoclasts, closing zone dominated by osteoblasts, and resting zone where osteoclasts and osteoblasts reached a balance. The osteoblast-to-osteocyte transformation is also shown. BMU, multicellular unit.

of endothelial reticulum and Golgi apparatus and the cellular secretion are reduced. In the meantime, osteoblast-specific markers like osterix, ALP, OCN, Cbfa1, and casein kinase II disappeared, while osteocyte markers like DMP-1, FGF23, ORP150, and Sost are highly expressed.^{21,74} To be noted, only a small ratio of osteoblasts is entrapped and transform into osteocytes,^{75,76} and other osteoblasts either become bone lining cells or undergo apoptosis. The entrapment ratio is correlated to the bone matrix secretory rate and the osteoblast burial rate, and varies with species, tissues, ages, and locations.⁷⁷

The incorporation of osteoblasts into bone matrix to become osteocytes is not a random process. Some researchers propose that osteoblast embedding is a passive process in which the osteoblasts are “buried alive” by the deposited matrix,⁷⁸ while others believe that the embedding is an active process that requires continuous collagen cleavage by matrix metalloproteinase.⁷⁹ A recent study using long-term time-lapse imaging technology demonstrated that these two theories were not exclusive, instead, they functioned side-by-side since the “buried alive” and “walk in” phenomena were observed simultaneously. Moreover, another phenomenon that cells already embedded in a lacuna started to differentiate *in situ* was also observed. Therefore, more than one mechanism participates in the osteoblast-to-osteocyte transformation process and its dominant mechanism can be different at different maturation stages.⁸⁰

A complex signaling network regulates the osteoblast-to-osteocyte transformation process, and the signals from osteocytes play critical roles during this process. *In vitro* co-culture study showed that when osteocytes were exposed to mechanical stress (fluid flow stress), osteocytes released signals to co-cultured osteoblasts and induced osteoblast differentiation. When the fluid flow was directly applied to the osteoblasts, the differentiation of the osteoblasts failed to occur.⁸¹ Mathematical models implied osteocyte signals come from a large group of osteocytes rather than only those closest to the bone deposition front.⁷⁷ Although the exact molecular mechanism underneath the transformation remains unclear, many bioactive factors have been identified, including MMPs, DMP1, OF45/MEPE, klotho gene, TGF- β inducible early gene-1 (TIEG), LPA, E11, and oxygen.¹⁶ Intracellular communication through direct cell-cell junctions also participates in this transformation. A large amount of adherens junction, gap junction,⁸² and tight junction⁸³ were observed between the osteocyte dendrites and osteoblasts, as well as between the dendrites from adjacent osteocytes. These junctions,⁸⁴ especially gap junction,⁸⁵ have been proved to play critical roles in osteocyte-osteoblast communication. Moreover, cell-cell interaction through ligand-receptor interactions, such as Notch^{86,87} and Ephrin-Ephrin receptors,⁸⁸ was found on the plasma membranes of osteoblasts and osteocytes. Therefore, secretory signals, intracellular junctions, and the ligand-receptor-mediated cell-cell interactions form a complicated signaling network that regulates the osteoblast-to-osteocyte transformation and bone modeling/remodeling process.^{84,89}

Microdamage

Microdamage in bone occurs due to repetitive mechanical loading in daily life. Mechanical loading changes both the

chemical composition and the crystal structure of the bone mineral⁹⁰ and leads to the formation of microdamage. In physiological conditions, microdamage is normally present in bone and functions as a stimulus to induce local bone remodeling. However, not all microdamage is repaired.⁹¹ In aged or pathological bone, the rate of bone remodeling slows down and microdamage accumulates. The accumulation of microcracks not only impacts the mechanical strength of bone by decreasing its elastic modulus, ultimate strength, and mechanical energy-absorbing ability but also impairs its fracture toughness, making the bone less resistant to fractures.^{90,92}

The microdamage can be divided into linear microcracks and diffuse damages, which differ in various aspects, including morphology, location, inducing stress, and repair mechanisms.⁹³ Linear microcracks have sharp borders and are larger than canaliculi, but smaller than vascular canals in 2D histomorphology,⁹⁰ while their actual 3D morphology is an elliptical shape that orients $\sim 20^\circ$ from the longitudinal axis of cortical bone.⁹⁴ Meanwhile, the lengths of microcracks usually exceed 10 μm . Diffuse damages appear as clouds of stain with indistinguishable individual features in 2D histomorphology, while they indeed comprised many smaller cracks that occur below the lamellar length scale (1–3 μm) or even at the level of the collagen fibril (<1 μm). The morphology of the diffuse damages indicates that they are more capable of dissipating energy, which was verified by the fact that they are more commonly seen in younger bone, whereas linear microcracks are more commonly seen in older bone. Besides, diffuse damages are more prominent when tensile forces are applied, while linear microcracks are mainly caused by compressive forces.⁹⁵ Moreover, the repair of diffuse damages is also distinct from that of linear microcracks.^{96,97} In contrast to linear microcracks that require osteocyte-mediated BMU remodeling, diffuse microdamage can be self-repaired. This self-repair process can be explained by a sacrificial bonds theory that the ionic bonds in the collagen matrix are broken by an external force and is repaired at the molecular level when the force is removed; or by an annealing theory that the components of the organic matrix bridge very small cracks and provide resistance to crack growth.⁹³ It was reported that microcrack propagation was more deleterious than microcrack initiation⁹⁸; thus, diffuse damages that seldom propagate usually do not cause substantial damages to bone.

Osteocytes are believed as the cellular components that sense and respond to bone microdamage, and the mechanism underlying this process has been discussed for years.⁹⁹ One theory states that microcracks lead to osteocyte cellular change directly. During crack opening and shear displacements, microcracks cause rupture of osteocyte dendrites,⁹⁴ which subsequently results in osteocyte apoptosis.¹⁰⁰ The length of microcracks determines the stress threshold that induces dendrite rupture. A short microcrack corresponds to a high strain threshold so that the bone is less likely to fracture. One study reported that microcracks with a critical length of 91 μm corresponded to a typical peak physiological stress of 40 MPa; therefore, microcracks shorter than the threshold length would not cause any noticeable damage to osteocyte dendrites.⁹⁴ Apoptotic osteocytes send signals to adjacent viable osteocytes that release RANKL from the membrane surfaces to activate osteoclastogenesis and

initiate the local bone remodeling process.^{101,102} In this process, not only osteocyte apoptosis¹⁰¹ but also mechanical loading¹⁰³ is indispensable to activate osteoclast-initiated bone remodeling since either apoptosis-inhibited osteocytes or normal osteocytes deprived of mechanical stress fail to induce osteoclast activation. Another theory claims that microcracks lead to shear stress change in the LCN system. When this signal is perceived by osteocytes, a remodeling process is initiated and osteocyte apoptosis is not a necessary step. Although there is no technology available to directly measure bone fluid flow, mathematical models were developed to simulate this process.^{104–106} It was found that a fatigue microcrack can alter velocity and shear stress distributions as far as 150 μm away in the region,¹⁰⁵ and microcracks themselves can induce the release of fluid pressure and increase the local liquid velocity upon load bearing.¹⁰⁴ The shape, size, and direction of microcracks influence the changes of pressure and velocity, which function as a signal to nearby osteocytes. Another study further supported this theory by proving that mechanical loading directly induced osteoclast and osteoblast functions without inducing osteocyte apoptosis.⁶⁸

Osteons are generally regarded as an effective adaption to inhibit microcrack growth and fracture occurrence owing to the cement line, although the collagen fiber-mineral ultrastructure could encourage the formation of numerous nonpropagating small cracks.¹⁰⁷ The length of microcracks reflects the energy it contains during microcrack growth, and plays a determinative role in its interaction with osteons. Short microcracks are usually less energetic and cease as they hit an osteon, and those with intermediate lengths are deflected around cement lines toward a path of least resistance. Long microcracks are self-propagating and can penetrate cement lines and damage the integrity of the osteonal structure. For those long microcracks, the concentric lamellae of osteons inversely function as a weakness and promote fracture propagation along the lamellae interface within the osteons.⁷

Osteon turnover in response to aging

Aging produces deleterious effects to bone. Although these effects are less severe to cortical bone than to trabecular bone, they damage the mechanical strength of bone since a small decrease of cortical bone can impose a significant impairment to the mechanical property of the bone. The mechanical strength of bone decreases and the rate of bone turnover slows down with aging. The thickness of cortical bone decreases with aging, owing to decelerated bone remodeling, especially at the endosteal side where bone resorption is more pronounced; therefore, the volume of the medullary cavity increases.

Aged bone usually displays a higher osteon density than young bone. This is possibly caused by the fact that the endosteal side where large and less denser osteons exist is more likely to be absorbed than the periosteal side.¹⁰⁸ Therefore, the osteon size decreases^{109,110} and the proportion of extra-Haversian bone increases.¹¹⁰ Aging also influences the shape of osteons and the average circularity index increases with age.¹⁰⁹ The density of Haversian canals that deliver osteoclast and osteoblast progenitors to the interior of cortical bone increases with age.¹¹⁰ The sizes of

those canals increase with age too, especially near the endosteal site where the canals tend to coalesce and form a cancellous-like architecture.¹¹¹ Consequently, the bone mineral density decreases and the cortical porosity increases. The turnover rate of aged bone decreases dramatically, owing to the lower bone remodeling capacities of osteoclasts and osteoblasts and declined levels of signals from osteocytes.

Lacuna density decreases and osteocyte destruction increases in aged osteons.¹¹² Osteocyte apoptosis occurs within the lacuna and the lacunocanicular space is completely hypermineralized,¹¹³ which is caused by the factors including reactive oxygen species accumulation, hyperglucocorticoidism, and failure in osteocyte autophagy.¹¹¹ Osteocytes also undergo autophagy, cannibalize themselves, and use their own proteins and lipids as metabolic energy supply. The self-destruction helps sustain cell survival in a nutrition-challenging or stress-concentrating microenvironment.¹¹⁴ Therefore, it is regarded as an approach to prolong tissue lifespan. In aged bone, osteocyte autophagy level decreased, and this decline may contribute to age-related bone loss since a significant correlation between the levels of osteocyte autophagy markers and bone mineral density was reported.¹¹⁵

Aging also influences the LCN system. It is demonstrated that osteocyte lacunae own the capacity of amplifying local tissue strains that are conducted to osteocytes.¹¹⁶ Therefore, a minor change in the LCN can significantly affect the local mechanical properties of bone. The morphology of osteocyte lacunae is affected by aging and becomes smaller in volume and more spherical in shape.¹¹⁷ The decrease of the LCN volume, as a result of declined lacuna density and declined lacuna volume, disturbs bone fluid flow and impairs the mechanosensation and mechanotransduction within an osteon. Moreover, the average number of canaliculi originated from each lacuna is also decreased, which further decelerates the fluid flow and impedes the signal transduction between osteocytes.¹¹⁸

Aging also influences bone quality indirectly by accumulating microdamage and increasing the level of glucocorticoids. Fatigue-induced microdamage normally appears in bone and functions as a stimuli for bone remodeling. A balance in bone quantity is usually maintained in healthy bone, while aging breaks this balance in several ways. A higher frequency of microdamage, especially in the form of linear microcracks, is observed in aged bone. The accumulation of microcracks decreases the fatigue resistance of bone, making it more difficult to resist regular level of mechanical stress. Besides, the mineralization level of cement lines and the surrounding bone matrix tends to be similar with aging; therefore, the capacity of cement lines to deflect microcracks decreases. As a result, microcracks are more likely to penetrate the cement line and destroy the integrity of osteons. In aged bone, small microcracks propagate with much less resistance and fuse into larger cracks that lead to bone fracture more easily.¹¹² Moreover, aged individuals tend to have a higher level of glucocorticoids than young individuals since the synthesis of adrenocorticotrophic hormone that suppresses glucocorticoid production through negative feedback is decreased. Hyperglucocorticoidism weakens bone quality by suppressing bone formation, increasing bone resorption, and promoting osteoblast and osteocyte apoptosis.¹¹⁹

Osteon Regeneration

Ever since the concept of tissue engineering was brought up in the 1980s, numerous studies focusing on bone regeneration have been performed, which have vastly contributed to the advancement of the clinical treatments of bone loss. However, cortical bone regeneration has never been achieved and the morphological features of osteons have not been observed within the regenerated bone tissues. In recent years, researchers have attempted to develop novel cytological tools and tissue engineering approaches to recapitulate the structure of cortical bone. In this part, studies that aimed at replicating the osteon elements are summarized.

Osteocytes and the LCN

As discussed previously, osteocytes and the LCN network play critical roles in bone function, especially the mechanosensation and mechanotransduction of bone. In conventional bone regeneration strategies, osteogenic stem cells or osteoblastic progenitor cells are routinely used that they gradually transform into osteocytes, accompanying the deposition of osteoid matrix. For cortical bone regeneration, this remodeling process is time-consuming; thus, the critical functions of osteocytes and the LCN network cannot be obtained timely. Recent advancement in cytological tools and scaffolding approaches has enabled the acceleration of osteoblast-to-

osteocyte transformation and the direct exploration of osteocytes *in vitro*. In this study, a summary of these strategies is presented, which hopefully will provide hints for accelerating cortical bone regeneration (Fig. 4).

Osteocyte-like cell lines. Osteocytes are terminally differentiated cells and lose the capacity of proliferation. To explore the physiological behavior of osteocytes, the mechanosensation/mechanotransduction function, and the osteoblast-to-osteocyte transition process, researchers have established several clonal cell lines by immortalization of primary bone cells. Those cell lines not only maintain cell proliferation capacity but also express genetic profiles similar to osteocytes. Commonly used cell lines include osteocyte-like MLO-Y4¹²⁰ and OCY454,¹²¹ post-osteoblast/pre-osteocyte MLO-A5,¹²² post-osteoblast-to-late osteocyte IDG-SW3,¹²³ and pre-to-late osteocyte OmGFP66.¹²⁴ Among them, MLO-A5, IDG-SW3, and OmGFP66 exhibit pre-osteocyte or osteoblast-like properties and are capable of secreting osteoid matrix, while maintaining osteocyte-specific properties. For example, both MLO-A5 and IDG-SW3 expressed high levels of alkaline phosphatase (ALP), secreted collagen, and formed mineralization. However, none of those cell lines can recapitulate the lacunocanalicular structure of nature bone. Recently, a novel OmGFP66 cell line that formed an organized *in vivo* bone-like lacunocanalicular structure was reported.¹²⁴ As the first cell line that is capable of replicating the physiological LCN of bone, the OmGFP66 provides a promising tool to explore the regeneration of cortical bone.

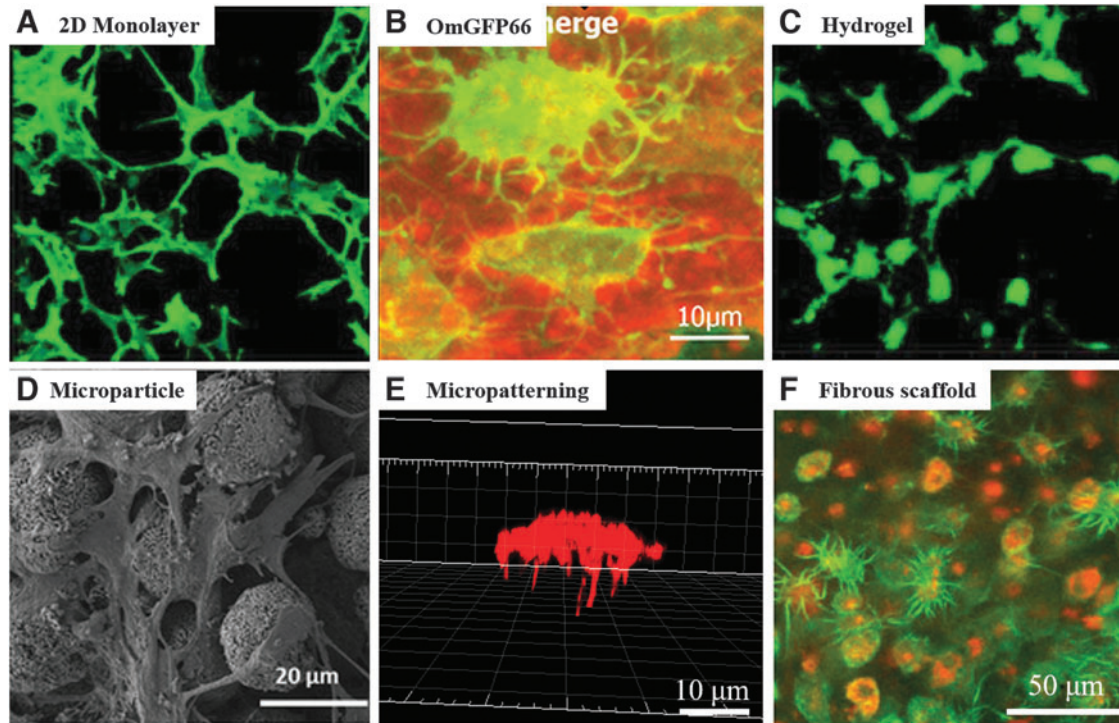


FIG. 4. *In vitro* culture strategies recapitulating osteocytic morphologies. (A) IDG-SW3 cells cultured in a 2D single layer, modified with permission from Yang *et al.*¹²⁵ (B) OmGFP66 cell line and the LCN, modified with permission from Wang *et al.*¹²⁴ (C) IDG-SW3 cells cultured within a 3D gelatin hydrogel, modified with permission from Yang *et al.*¹²⁵ (D) MLO-A5 cells cultured with biphasic calcium phosphate microparticles, modified with permission from Gu *et al.*¹³⁹ (E) Single BMSC cultured on a 3D tubular microisland, modified with permission from Ma *et al.*¹⁴¹ (F) Primary osteoblasts cultured within a 3D collagen fibrous scaffold, modified with permission from Matsugaki *et al.*¹⁴⁴ LCN, lacunocanalicular network.

Three-dimensional culture systems for osteocyte-like cells. While 2D monolayer culture is the most commonly used culture system for osteocytes or osteocyte-like cell lines, it fails to replicate the 3D physiological structure of osteocytes *in vivo*. As a result, the transformation from osteoblasts to osteocytes cannot be achieved. A 3D culture system that mimics the physiological condition is favorable to osteocytic differentiation. A summary of the 3D *in vitro* culture systems for osteocytic differentiation is provided in this section.

Hydrogels. Hydrogels have been widely used for osteocyte culture and osteoblast-to-osteocyte transformation exploration. Primary osteocytes or osteocyte-like cell lines exhibited a fibroblast-like spindle morphology when cultured on a 2D tissue culture polystyrene and failed to express osteocyte-related markers.¹²⁵ When those cells were suspended in a 3D gel construct, the physiological characteristics of *in vivo* osteocytes were well preserved that cells displayed a satellite morphology with elongated and communicable dendrites, expressed high level of osteocytic markers (E11, DMP-1, Sost, and Fgf 23), and presented a proliferation-ceased and mineralization-suppressive status.¹²⁵ More importantly, 3D hydrogels facilitated the transformation of osteoblasts/osteoblast-like cells to osteocytes, which was indicated by the elongated cellular processes, reduced ALP level and mineralization activity, and increased expression of osteocytic markers.^{126–128} Moreover, when the differentiated osteocytes were retracted from the 3D construct and cultured on a 2D surface, dedifferentiation occurred and the cells lost the dendritic morphology and expressed high level of osteoblastic marker genes.¹²⁷

Most hydrogels used for osteocytes are developed from collagen^{126–131} and gelatin,^{125,132,133} and occasionally Matrigel is used.^{130,134} The components of the hydrogel affect osteocytic behaviors. For example, adding type I collagen to a 3D gelatin gel significantly increased the number, length, and connections of osteocyte dendrites, the expression level of osteocytic markers, and the responsiveness to PTH.¹²⁵ A collagen gel that contained nanocrystalline hydroxyapatite shortened the osteocyte dendrites and decreased the ALP expression level compared to non-mineralized collagen gels.¹²⁹

The stiffness of a hydrogel plays a role in regulating osteocytic behaviors as well. A lower stiffness had advantageous effects in promoting the osteocytic differentiation of osteoblastic MC-3T3 cells, which was indicated by the formation of interconnected dendrite network,¹³² the down-regulation of ALP activity and osteoblastic genes (Col1 and OSF-2), and the upregulation of osteocyte-related genes (DMP-1 and Sost).¹³³ Similar trend was observed when the osteoblastic cells were cultured in a 3D gelatin hydrogel¹³² and on the surface of a collagen hydrogel.¹³³

Microparticles. Microparticles are also used for osteocytic culture.^{128,135–139} In one study, primary osteoblasts were mixed with biphasic calcium phosphate (BCP) microparticles that mimicked the mineral composition of bone matrix and presented a 3D culture environment to the osteoblasts.¹³⁵ Within the interstitial space between microparticles, the osteoblasts were embedded in the lacunae-like spaces surrounded by the cell-secreted osteoid matrix.

Moreover, the osteocytic marker genes were highly expressed and osteoblastic marker genes like ALP, osteonectin, and Col1 were downregulated, indicating a successful transition from osteoblasts to osteocytes. Besides, when polyethylene microparticles were added to a collagen gel, those microparticles presented a significant effect in inducing the osteocytic morphological transition and a catabolic phenotypic profile of primary osteoblasts compared to the use of pure collagen gel.¹²⁸

BCP microparticle culture system was improved with a decrease in microparticle size and the addition of a microfluidic perfusion, which facilitated the entrapment of single cells and the extension and connection of cell dendrites within the interstitial spaces. In the meantime, cell proliferation was mitigated, cell-cell distance was maintained, and osteocytic genes were upregulated, indicating that a more *in vivo*-like microenvironment was established.^{136–139}

Micropatterning. Micropatterning has also been used for inducing osteocytic differentiation. One study used a microcontact printing technique to create a micropatterned network to mimic the *in vivo* interconnected osteocyte LCN network.¹⁴⁰ The surface of a cover slide was divided into fibronectin-coated cell-adhesive regions and cell-repellent regions that were formed by ethylene glycol terminated self-assembled monolayer ink. The cell-adhesive regions included dispersedly organized circular regions that allowed bone cell attachment, and interconnected lines between the circles that supported the formation of cell dendrites. MC 3T3 cells attached on the circular regions were cultured separately and cell dendrites formed within the interconnected lines. Moreover, gap junctions were detected between the cells in the micropatterned network, indicating that cell-cell communication within the network was established. However, this micropatterning platform only allows cell-cell interactions on a 2D surface.

Our laboratory recently developed a nanofibrous micropatterned 3D platform to recapitulate the 3D dendritic morphology of osteocyte *in vitro*.¹⁴¹ The bioinspired 3D platform was generated by integrating the processes of nanofabrication, micropatterning, and computer-assisted laser ablation. A gelatin-based nanofibrous matrix fabricated by electrospinning was used as the substrate for a photolithography process, which generated isolated gelatin-exposed cell-adhesive microislands surrounded by polyethylene glycol-coated cell-repellent regions. Afterward, multiple bone canaliculi-like microchannels were created within the microislands by laser ablation. Single bone marrow stem cells (BMSC) cultured on the microislands displayed an osteocyte-like morphology that the satellite-like cell body resided on the microisland and multiple dendrites extended into the microchannels. By tailoring the parameters of micropatterning and laser ablation, we successfully made the cell body and dendrites of the BMSCs on the micropatterned 3D platform identical to those of osteocytes *in vivo*.

Fibrous scaffolds. It has been well known that the fibrous structure, which possessed a remarkably higher surface-to-volume ratio, presented a preferable effect to osteoblastic differentiation than a smooth surface.^{142,143} Therefore, fibrous scaffolds have been widely used for bone regeneration. However, most of the studies focused on the functional

differentiation of osteogenic cells, and very few of them explored the osteoblast-to-osteocyte transformation or the morphological maturation of osteocytes.

When a single BMSC was cultured on a micropatterned nanofibrous matrix, multiple filopodia with an average diameter similar to osteocyte dendrites invaded into the interconnected pores of the nanofibers.¹⁴¹ Recently, a 3D fibrous scaffold was developed using a 3D printing technique to extrude collagen fibers. Osteoblasts were seeded on the surface and migrated inside the scaffold. It was shown that the osteoblasts on the upper surface of the scaffold barely expressed sclerostin, while those embedded inside the scaffold expressed high level of sclerostin. Moreover, the embedded osteoblasts displayed an osteocyte-like morphology with multiple dendritic processes.¹⁴⁴ The results indicated that fibrous structure facilitated the differentiation of osteoblastic cells into osteocytes.

The orientation of the nanofibers played critical roles in maneuvering cell morphology. When cultured on 2D aligned nanofibers^{145,146} or within 3D layer-by-layer nanofibrous construct,¹⁴⁵ osteoblastic cells displayed a distinctly elongated morphology parallel to the orientation of the nanofibers compared to that on/within the random nanofibers. Moreover, cells extended processes (lamellipodia) along the nanofibers, which were steered by filopodia that act as cellular antennae to sense the substrate topography.¹⁴⁶ Meanwhile, the mineralized bone matrix produced by the osteoblasts also corresponded to the orientation of the underlying substrate.^{144,147} However, the effect of nanofiber orientation on the differentiation of osteogenic cells remains controversial.^{145,147}

Regulatory factors. In addition to cell types and scaffolding structures, many other factors also participate in the regulation of osteocytic differentiation and can be employed for cortical bone regeneration. Both *in vitro* studies^{18,148,149} and *in vivo* mice models¹⁸ have shown that mechanical load plays critical roles in inducing osteocytic differentiation. A microfluidic perfusion system that exerted controlled fluid

flow stress to osteoblastic cells was developed to replicate the mechanotransduction network of bone.¹³⁷ Cell density is another biophysical factor that influenced osteocyte differentiation, although its exact effect remains debatable. Two studies reported that a higher cell density was advantageous in promoting the morphological transformation, dendrite formation, and mineralization of osteoblastic cells,^{132,150} while one study showed opposite results.¹³³ Considering that the cell density and culture environment used in those studies were not consistent, more comprehensive work is needed to address the contradicted results.

One important biochemical factor that regulates osteocytic differentiation is oxygen tension. The physiological microenvironment where osteocytes reside is hypoxic.¹⁵¹ Multiple *in vitro* studies have indicated that a low oxygen tension is preferable for osteoblast-to-osteocyte transformation.^{138,151,152} Other factors like calcium,¹⁵³ strontium,^{129,154} vitamin K,¹³¹ and 1,25-dihydroxyvitamin D3¹⁵⁵ also exhibited positive effects in inducing osteocytic differentiation, while PTH induced the loss of mature osteocyte phenotype.¹⁵⁶

Lamellae

Within the context of osteon regeneration, two approaches have been attempted to mimic the concentric osteon lamellae. One is the 3D printing technique. In one study,¹⁵⁷ two syringes were used to generate a cylindrical multicircular scaffold. For the innermost layer, a mixture of fibrinogen/gelatin/human umbilical vein endothelial cells (HUVECs) was used as bioink to mimic the structure of Haversian canal. For the outer several layers, the bioink encapsulating fibrinogen/gelatin/mesenchymal stem cells was used to mimic bone matrix. However, when the scaffold/cell construct was cultured *in vitro* or implanted *in vivo*, the boundaries between the layers disappeared and could not mimic lamella structure. The other approach combines electrospinning and a rolling process to fabricate lamella structure (Fig. 5). During the fabrication process,

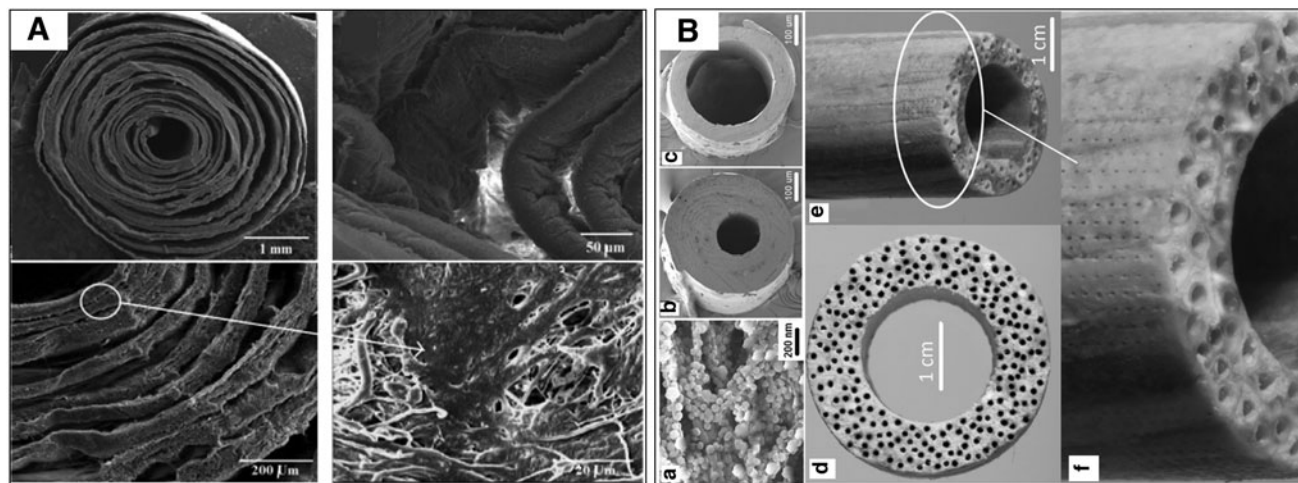


FIG. 5. The application of electrospinning and rolling techniques in recapitulating the osteon lamellae-like structure. (A) PCL/gelatin nanofibrous matrix with coral microparticles loaded between layers, showing the void space and the cells migrated inside, modified with permission from Hejazi and Mirzadeh.¹⁵⁹ (B) A cortical bone-mimicking scaffold generated by electrospinning, wrapping, annealing, and ultraviolet laser micro-drilling techniques. (a) The PLA microsheet composed of aligned nanofibers and CaP; (b) and (c) Cross-sectional image of a microtube with different ratios of wall thickness to outside radius; Cross-sectional image (d) and side-view (e) of a cortical scaffold prepared by fusion of microtubes; (f) Magnified side-view of (e) showing the array of microholes drilled on the outer surface. Adopted with permission from Barati *et al.*¹⁶⁰

a polymer solution was exposed to a high-voltage field to generate nanofibrous matrix and was rolled manually to form a 3D osteon-like construct. Compared to the 3D printing technique, this technique possesses advantages that the resultant constructs could replicate the nanofibrous structure of bone matrix, the lamella structure of osteons, and the osteocyte canaliculi owing to the pores formed by interweaving nanofibers. Moreover, the nanofibrous matrix can be soaked in simulated body fluid (SBF) for further mineralization.

One study used a commercial poly(glycolic acid) (PGA) fiber as the rotating stage to collect poly-L-lactide (PLLA) or PLLA/gelatin electrospun fibers.¹⁵⁸ In this construct, the PGA fiber was used as a core to mimic the Haversian canal and the outer electrospun fibrous layers were used to mimic the osteon lamellae. However, the result showed that the degradation rate of the PGA core was too slow and only a small portion of the PGA was degraded after 4 weeks of culture; thus, endothelial cells cannot be seeded in the center of the construct. Besides, osteogenic cells seeded on the construct were found only on the outermost surface, while orderly aligned osteocytes within the lamellae and the dendrites were not observed.

Another study proposed that the tight assembly of nanofibrous layers during the electrospinning process impaired cell migration.¹⁵⁹ Therefore, coral microparticles were repetitively attached to the nanofibrous layers after a certain time of electrospinning. In this way, void space between the layers was created to facilitate cell attachment. This work replicated the concentric lamellas and provided a clue for obtaining orderly aligned osteocytes.

In a recent study, one approach was employed to generate a construct similar to cortical bone.¹⁶⁰ First, nanofibrous PLA fabricated with an electrospinning technique was soaked into SBF for CaP nucleation. Next, the matrix was wrapped on a needle and annealed to fuse the nanofibrous layers. Afterward, the microtube-needle assemblies were formed around a stainless steel rod and further annealed to fuse the assemblies. After needles and the rod were removed, the spaces mimicking the Haversian canal and bone marrow were generated. A scanning deep-ultraviolet laser microdrilling system was used to drill microholes on the outer surface of the construct to mimic Volkmann canals. Although microstructural features of natural osteons such as the orderly aligned osteocytes and the dendrites were still missing in this system, it has proposed the feasible techniques to replicate the characteristics of natural osteons, including the nanofibrous architecture of bone matrix, osteon lamella, Haversian canals, and even Volkmann canals.

Haversian canals

The recapitulation of the Haversian canal, particularly the spatial arrangement of the Haversian canal and the surrounding bone matrix, is essential for osteon and cortical bone regeneration. Several techniques have been proposed to recapitulate this structure (Fig. 6).

Bottom-up methods. A bottom-up method is the most widely used approach to mimic osteon structure. This method is composed of two steps. First, a photocrosslinkable polymer solution was crosslinked with ultraviolet light

under a pre-designed concentric circular photomask to generate “double-ring” microgels. The polymer solution was composed of photocrosslinkable and biocompatible materials such as polyethylene glycol diacrylate,¹⁶¹ GelMA,^{162,163} and RGD-modified alginate.^{164,165} The hydrogel used for the inner ring contained endothelial cells like HUVECs, while the hydrogel used for the outer rings contained osteogenic cells like MG63 or BMSCs. Since the thickness of the microgels usually did not exceed 500 μm , a second step was needed and the microgels were assembled in a layer-by-layer manner and crosslinked with ultraviolet light to eliminate the gap between the layers. In this way, a 3D tube-like construct with a spatial arrangement of endothelial cells and osteogenic cells was formed. The two types of cells directly communicated with each other, leading to enhanced angiogenesis of the endothelial cells and osteogenesis of the osteogenic cells.^{162,163,166}

Casting. One study used a casting technique to generate a 3D nanocrystalline HA scaffold.¹⁶⁷ This scaffold had a honeycomb pore architecture formed by parallelly aligned microchannels, which were used to mimic the Haversian canals. *In vitro* evaluations showed that this scaffold promoted monocytes to differentiate into osteoclasts, and enhanced osteoblast proliferation and differentiation. An *in vivo* cortical bone defect model showed it effectively recruited osteogenic cells to the microchannels and promoted the secretory function and even the osteon-like bone formation. Although endothelial cells and vascularization were not evaluated in that work, the authors proposed that the scaffold might guide blood vessel invasion and facilitate revascularization *in vivo* structurally.

Extrusion. An extrusion process has also been employed to generate the Haversian canals and the osteon-mimicking scaffolds. One study designed a shell-core bilayered scaffold with a combination of electrospinning and a twin screw extrusion process.¹⁶⁸ A hollow polycaprolactone (PCL) nanofibrous tube was fabricated with the electrospinning technique and used as a core to mimic the Haversian canal. Then a polycaprolactone/biphase calcium phosphate (PCL/BCP) mixture was extruded surrounding the PCL core to form the coil-like shell to mimic bone matrix. Endothelial cells were seeded within the PCL tube and pre-osteoblasts were seeded on the exterior surface of the PCL/BCP shell. The nanofibrous inner surface of the PCL core promoted the confluence of endothelial cells, which formed a continuous lining layer with intercellular tight junctions. Meanwhile, the coil-like shell enhanced pre-osteoblast proliferation and differentiation. Although the spatial arrangement of the Haversian canal was mimicked and vascularization and osteogenesis were enhanced, this work failed to obtain a direct interaction between endothelial and osteogenic cells.

Another study designed a multichannel microfluidic system that enabled the spatial organization of HUVECs and MG63 cells.¹⁶⁹ An osteon-like microfiber were composed of four layers of components, which were extruded sequentially and assembled on a pre-designed photolithography-based microfluidic chip. The innermost layer was formed by hyaluronic acid, which was dissolved in water to create the hollow structure to mimic the Haversian canal. The second and third layers were formed by HUVEC-loaded RGD-alginate and MG63-loaded RGD-alginate hydrogel, respectively. The outermost

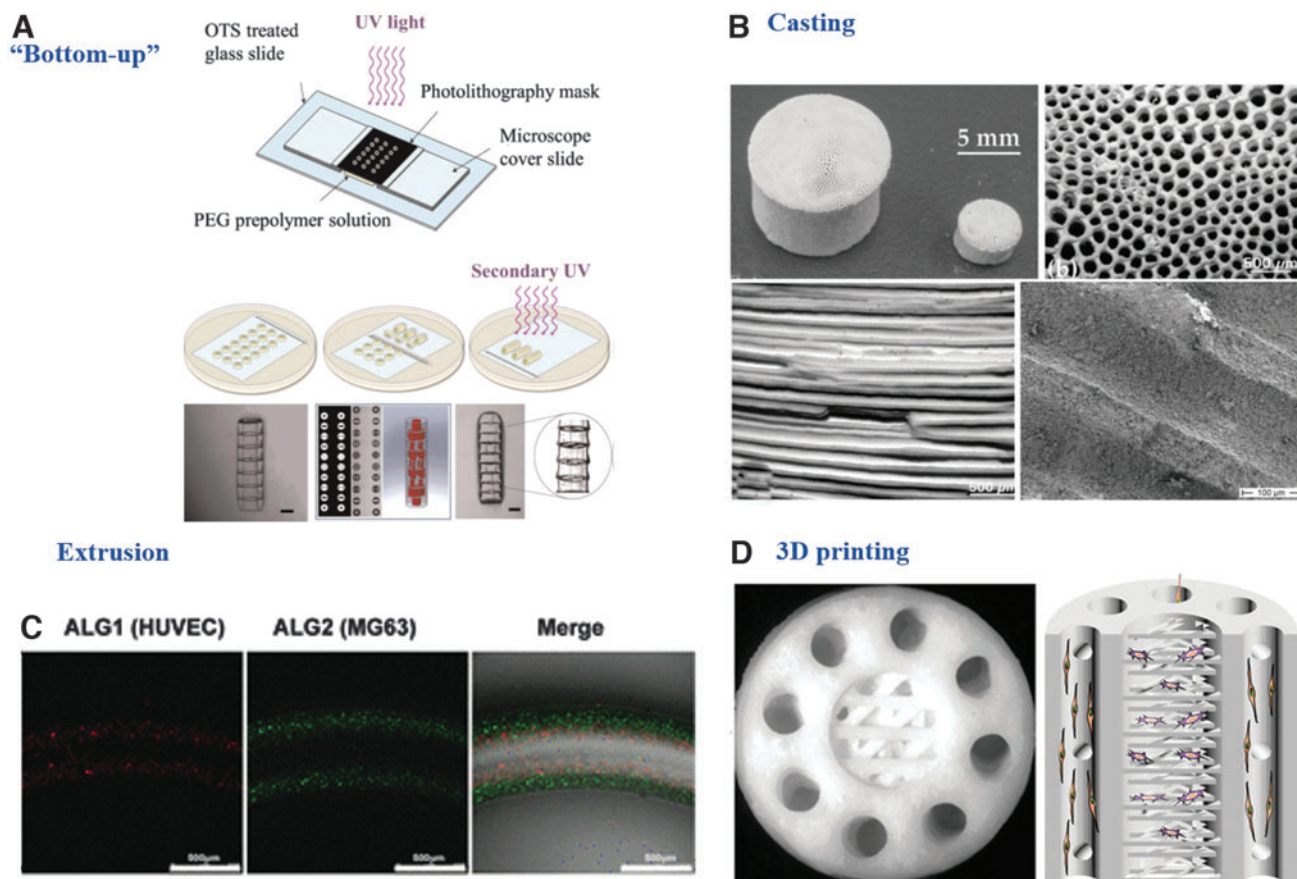


FIG. 6. Strategies recapitulating the Haversian canal or the spatial organization of Haversian canal and bone matrix. (A) “Double-ring” microgels assembled layer-by-layer by a “Bottom-up” technique, modified with permission from Du *et al.*¹⁶¹ (B) Replication of cortical bone by a casting technique, modified with permission from Despong *et al.*¹⁶⁷ (C) Spatial cell-laden fibers by an extrusion technique, modified with permission from Wei *et al.*¹⁶⁹ (<https://pubs.acs.org/doi/10.1021/acsami.7b00078>). Further permissions related to the material excerpted should be directed to the ACS). (D) Replication of cortical bone by 3D printing, modified with permission from Zhang *et al.*¹⁷⁰

layer was water to ensure the integrity of the microgels. In this way, the microfibers recapitulated the structure of the Haversian canal and bone matrix, enabling a direct communication between endothelial and osteogenic cells.

Three-dimensional printing. The 3D printing is another technique to recapitulate Haversian canal. Apart from organic bioink to print the innermost layer to mimic the Haversian canal as aforementioned,¹⁵⁷ researchers also used inorganic ink for 3D printing. In one study, an akermanite bioceramic ink was used in a digital laser processing-based 3D printer to replicate the structure of an osteon.¹⁷⁰ This scaffold recapitulated the structure of the Haversian canals, Volkmann canals, and cancellous bone together with the physiological spatial arrangement. Moreover, the growth of human bone marrow stem cells in the cancellous structure and HUVECs on the Haversian canal of the scaffold efficiently enhanced osteogenic and angiogenic differentiation.

Conclusions and Future Perspectives

Osteons in cortical bone have aroused enormous interest ever since the discovery. The microstructural components of an osteon, including its lamellae, osteocytes, LCN, and

Haversian canal, form a delicately communicative network that supports the physiological function and turnover of cortical bone. Massive studies have been conducted to explore the role of each indispensable component and their interactions, which have greatly contributed to the knowledge of osteons. The development of advanced imaging techniques and mathematical models further facilitate our in-depth understanding of osteons. However, many questions, including the cause of alternating morphology of lamellae and the molecular mechanism underlying osteocyte mechanosensation and mechanotransduction, remain unsolved and require future exploration.

The final part of this review summarizes the development of bioengineering approaches to recapitulate the osteon structure. Osteons form the functional units of cortical bone, and successful recapitulation of the osteon structure builds the foundation of cortical bone regeneration. If bioinspired osteon-like scaffolds can be designed and directly induce cortical bone formation, the postsurgical rehabilitation time for orthopedic surgery patients will be dramatically reduced. From this point of view, the regeneration of cortical bone in orthopedic research is of clinical significance. To date, the development of such bioinspired scaffolds to regenerate osteons and cortical bone is still in its infancy and the

expansion of this research will enable development of new therapies for reconstructive orthopedics.

Disclosure Statement

No competing financial interests exist.

Funding Information

This research was supported by National Institute of Dental and Craniofacial Research (NIDCR) grant numbers DE024979 and DE029860 (XL).

References

- Campana, V., Milano, G., Pagano, E., *et al.* Bone substitutes in orthopaedic surgery: from basic science to clinical practice. *J Mater Sci Mater Med* **25**, 2445, 2014.
- Greenwald, A.S., Boden, S.D., Goldberg, V.M., Khan, Y., Laurencin, C.T., and Rosier, R.N. Bone-graft substitutes: facts, fictions, and applications. *JBJS* **83**, S98, 2001.
- Zimmermann, G., and Moghaddam, A. Allograft bone matrix versus synthetic bone graft substitutes. *Injury* **42**, S16, 2011.
- Cancedda, R., Giannoni, P., and Mastrogiacomo, M. A tissue engineering approach to bone repair in large animal models and in clinical practice. *Biomaterials* **28**, 4240, 2007.
- Carter, C.B., and Norton, M.G. *Ceramic Materials: Science and Engineering*. Berlin, Germany: Springer, 2007.
- Magal, R.A., Reznikov, N., Shahar, R., and Weiner, S. Three-dimensional structure of minipig fibrolamellar bone: adaptation to axial loading. *J Struct Biol* **186**, 253, 2014.
- Mohsin, S., O'Brien, F.J., and Lee, T.C. Osteonal crack barriers in ovine compact bone. *J Anat* **208**, 81, 2006.
- Weiner, S., Traub, W., and Wagner, H.D. Lamellar bone: structure–function relations. *J Struct Biol* **126**, 241, 1999.
- Martiniaková, M., Grosskopf, B., Vondráková, M., Omelka, R., and Fabiš, M. Observation of the microstructure of rat cortical bone tissue. *Scripta Med* **78**, 45, 2005.
- An, Y.H., and Draughn, R.A. *Mechanical Testing of Bone and the Bone-Implant Interface*. Boca Raton, FL: CRC Press, 1999.
- Schwarz, H.P., Abueidda, D., and Jasiuk, I. The ultrastructure of bone and its relevance to mechanical properties. *Front Phys* **5**, 39, 2017.
- Robling, A.G., and Stout, S.D. Morphology of the drifting osteon. *Cells Tissues Organs* **164**, 192, 1999.
- Raguin, E., and Streeter, M.A. Brief communication: test of a method to identify double-zonal osteon in polarized light microscopy. *Am J Phys Anthropol* **167**, 407, 2018.
- Power, J., Doube, M., van Bezooijen, R.L., Loveridge, N., and Reeve, J. Osteocyte recruitment declines as the osteon fills in: interacting effects of osteocytic sclerostin and previous hip fracture on the size of cortical canals in the femoral neck. *Bone* **50**, 1107, 2012.
- Milovanovic, P., Zimmermann, E.A., Hahn, M., *et al.* Osteocytic canalicular networks: morphological implications for altered mechanosensitivity. *ACS Nano* **7**, 7542, 2013.
- Noble, B.S. The osteocyte lineage. *Arch Biochem Biophys* **473**, 106, 2008.
- Tanaka-Kamioka, K., Kamioka, H., Ris, H., and Lim, S.S. Osteocyte shape is dependent on actin filaments and osteocyte processes are unique actin-rich projections. *J Bone Miner Res* **13**, 1555, 1998.
- Zhang, K., Barragan-Adjemian, C., Ye, L., *et al.* E11/gp38 selective expression in osteocytes: regulation by mechanical strain and role in dendrite elongation. *Mol Cell Biol* **26**, 4539, 2006.
- Goldring, S.R. The osteocyte: key player in regulating bone turnover. *RMD Open* **1**, e000049, 2015.
- Bellido, T. Osteocyte-driven bone remodeling. *Calcif Tissue Int* **94**, 25, 2014.
- Capulli, M., Paone, R., and Rucci, N. Osteoblast and osteocyte: games without frontiers. *Arch Biochem Biophys* **561**, 3, 2014.
- Rocheffort, G.Y., Pallu, S., and Benhamou, C.-L. Osteocyte: the unrecognized side of bone tissue. *Osteoporos Int* **21**, 1457, 2010.
- Tsourdí, E., Jähn, K., Rauner, M., Busse, B., and Bonewald, L.F. Physiological and pathological osteocytic osteolysis. *J Musculoskelet Neuronal Interact* **18**, 292, 2018.
- Bakker, A.D., and Klein-Nulend, J. Mechanisms of osteocyte mechanotransduction. *Clin Rev Bone Miner Metab* **8**, 163, 2010.
- Nguyen, A.M., and Jacobs, C.R. Emerging role of primary cilia as mechanosensors in osteocytes. *Bone* **54**, 196, 2013.
- Geoghegan, I.P., Hoey, D.A., and McNamara, L.M. Integrins in osteocyte biology and mechanotransduction. *Curr Osteoporos Rep* **17**, 195, 2019.
- Lee, N.K., Sowa, H., Hinoi, E., *et al.* Endocrine regulation of energy metabolism by the skeleton. *Cell* **130**, 456, 2007.
- Metzger, C.E., and Narayanan, S.A. The role of osteocytes in inflammatory bone loss. *Front Endocrinol* **10**, 285, 2019.
- Charles, J.F., and Nakamura, M.C. Bone and the innate immune system. *Curr Osteoporos Rep* **12**, 1, 2014.
- Brun, J., Berthou, F., Trajkovski, M., Maechler, P., Foti, M., and Bonnet, N. Bone regulates browning and energy metabolism through mature osteoblast/osteocyte PPAR γ expression. *Diabetes* **66**, 2541, 2017.
- Sato, M., Asada, N., Kawano, Y., *et al.* Osteocytes regulate primary lymphoid organs and fat metabolism. *Cell Metab* **18**, 749, 2013.
- Price, C., Zhou, X., Li, W., and Wang, L. Real-time measurement of solute transport within the lacunar-canalicular system of mechanically loaded bone: direct evidence for load-induced fluid flow. *J Bone Miner Res* **26**, 277, 2011.
- van Hove, R.P., Nolte, P.A., Vatsa, A., *et al.* Osteocyte morphology in human tibiae of different bone pathologies with different bone mineral density—is there a role for mechanosensing? *Bone* **45**, 321, 2009.
- Milovanovic, P., and Busse, B. Inter-site Variability of the Human Osteocyte Lacunar Network: implications for Bone Quality. *Curr Osteoporos Rep* **17**, 105, 2019.
- Thompson, W.R., Modla, S., Grindel, B.J., *et al.* Perlecan/Hspg2 deficiency alters the pericellular space of the lacunocanalicular system surrounding osteocytic processes in cortical bone. *J Bone Miner Res* **26**, 618, 2011.

36. Weinkamer, R., Kollmannsberger, P., and Fratzl, P. Toward a connectomic description of the osteocyte lacuno-canalicular network in bone. *Curr Osteoporos Rep* **17**, 186, 2019.
37. Buenzli, P.R., and Sims, N.A. Quantifying the osteocyte network in the human skeleton. *Bone* **75**, 144, 2015.
38. Wittig, N.K., Laugesen, M., Birkbak, M.E., *et al.* Canalicular junctions in the osteocyte lacuno-canalicular network of cortical bone. *ACS Nano* **13**, 6421, 2019.
39. Tai, K., Dao, M., Suresh, S., Palazoglu, A., and Ortiz, C. Nanoscale heterogeneity promotes energy dissipation in bone. *Nat Mater* **6**, 454, 2007.
40. Hofmann, T., Heyroth, F., Meinhard, H., Fränzel, W., and Raum, K. Assessment of composition and anisotropic elastic properties of secondary osteon lamellae. *J Biomech* **39**, 2282, 2006.
41. Marotti, G. A new theory of bone lamellation. *Calcif Tissue Int* **53**, S47, 1993.
42. OTTI, G., Muglia, M., and Palumbo, C. Structure and function of lamellar bone. *Clin Rheumato* **13**, 63, 1994.
43. Marotti, G., Muglia, M.A., Palumbo, C., and Zaffe, D. The microscopic determinants of bone mechanical properties. *Ital J Miner Elect M* **8**, 167, 1994.
44. Mitchell, J., and van Heteren, A.H. A literature review of the spatial organization of lamellar bone. *C R Palevol* **15**, 23, 2016.
45. Burr, D.B., Schaffler, M.B., and Frederickson, R.G. Composition of the cement line and its possible mechanical role as a local interface in human compact bone. *J Biomech* **21**, 939, 1988.
46. Skedros, J.G., Holmes, J.L., Vajda, E.G., and Bloebaum, R.D. Cement lines of secondary osteons in human bone are not mineral-deficient: new data in a historical perspective. *Anat Rec A* **286**, 781, 2005.
47. Milovanovic, P., vom Scheidt, A., Mletzko, K., *et al.* Bone tissue aging affects mineralization of cement lines. *Bone* **110**, 187, 2018.
48. Dong, X.N., Zhang, X., and Guo, X.E. Interfacial strength of cement lines in human cortical bone. *MCB* **2**, 63, 2005.
49. Gupta, H., Stachewicz, U., Wagermaier, W., Roschger, P., Wagner, H., and Fratzl, P. Mechanical modulation at the lamellar level in osteonal bone. *Mater Res* **21**, 1913, 2006.
50. Montalbano, T., and Feng, G. Nanoindentation characterization of the cement lines in ovine and bovine femurs. *Mater Res* **26**, 1036, 2011.
51. Zimmermann, E.A., and Ritchie, R.O. Bone as a structural material. *Adv Healthc Mater* **4**, 1287, 2015.
52. O'Brien, F.J., Taylor, D., and Lee, T.C. The effect of bone microstructure on the initiation and growth of microcracks. *J Orthop Res* **23**, 475, 2005.
53. Marotti, G., and Zallone, A.Z. Changes in the vascular network during the formation of Haversian systems. *Cells Tissues Organs* **106**, 84, 1980.
54. Kim, J.-N., Lee, J.-Y., Shin, K.-J., Gil, Y.-C., Koh, K.-S., and Song, W.-C. Haversian system of compact bone and comparison between endosteal and periosteal sides using three-dimensional reconstruction in rat. *Anat Cell Biol* **48**, 258, 2015.
55. Pazzaglia, U.E., Congiu, T., Raspanti, M., Ranchetti, F., and Quacci, D. Anatomy of the intracortical canal system: scanning electron microscopy study in rabbit femur. *Clin Orthop Relat Res* **467**, 2446, 2009.
56. Deisseroth, K., and Hogan, H. Three dimensional modeling and analysis of Haversian systems in compact bone tissue. Presented at the "Proceedings of the 1995 Fourteenth Southern Biomedical Engineering Conference", Shreveport, LA, 1995, p.107.
57. Tappen, N. Three-dimensional studies of resorption spaces and developing osteons. *Am J Anat* **149**, 301, 1977.
58. Jaworski, Z. Haversian systems and haversian bone. *Bone Miner Metab* **4**, 21, 1992.
59. Qiu, S., Fyhrie, D.P., Palnitkar, S., and Rao, D.S. Histomorphometric assessment of Haversian canal and osteocyte lacunae in different-sized osteons in human rib. *Anat Rec A* **272**, 520, 2003.
60. Shapiro, F., and Wu, J. Woven bone overview: structural classification based on its integral role in developmental, repair and pathological bone formation throughout vertebrate groups. *Eur Cell Mater* **38**, 137, 2019.
61. Currey, J. The many adaptations of bone. *J Biomech* **36**, 1487, 2003.
62. Enlow, D.H. Functions of the Haversian system. *Am J Anat* **110**, 269, 1962.
63. Petrářl, M., Heřt, J., and Fiala, P. Spatial organization of the haversian bone in man. *J Biomech* **29**, 161, 1996.
64. Mayya, A., Banerjee, A., and Rajesh, R. Mammalian cortical bone in tension is non-Haversian. *Sci Rep* **3**, 2533, 2013.
65. Lin, Z.X., Xu, Z.-H., An, Y.H., and Li, X. In situ observation of fracture behavior of canine cortical bone under bending. *Mater Sci Eng C* **62**, 361, 2016.
66. O'Brien, F.J., Taylor, D., and Lee, T.C. Microcrack accumulation at different intervals during fatigue testing of compact bone. *J Biomech* **36**, 973, 2003.
67. Bentolila, V., Boyce, T., Fyhrie, D.P., Drumb, R., Skerry, T., and Schaffler, M.B. Intracortical remodeling in adult rat long bones after fatigue loading. *Bone* **23**, 275, 1998.
68. Van Oers, R.F., Ruimerman, R., Tanck, E., Hilbers, P.A., and Huiskes, R. A unified theory for osteonal and hemiosteonal remodeling. *Bone* **42**, 250, 2008.
69. Martínez-Reina, J., Reina, I., Domínguez, J., and García-Aznar, J. A bone remodelling model including the effect of damage on the steering of BMUs. *J Mech Behav Biomed Mater* **32**, 99, 2014.
70. Smit, T.H., Burger, E.H., and Huyghe, J.M. A case for strain-induced fluid flow as a regulator of BMU-coupling and osteonal alignment. *J Bone Miner Res* **17**, 2021, 2002.
71. Sims, N.A., and Martin, T.J. Osteoclasts provide coupling signals to osteoblast lineage cells through multiple mechanisms. *Annu Rev Physiol* **82**, 507, 2020.
72. Sims, N.A., and Martin, T.J. Coupling the activities of bone formation and resorption: a multitude of signals within the basic multicellular unit. *BoneKEY Rep* **3**, 481, 2014.
73. Lassen, N.E., Andersen, T.L., Pløen, G.G., *et al.* Coupling of bone resorption and formation in real time: new knowledge gained from human Haversian BMUs. *J Bone Miner Res* **32**, 1395, 2017.
74. Bonewald, L.F. The amazing osteocyte. *J Bone Miner Res* **26**, 229, 2011.
75. Hadjidakis, D.J., and Androulakis, I.I. Bone remodeling. *Ann N Y Acad Sci* **1092**, 385, 2006.
76. Pazzaglia, U.E., Congiu, T., Sibilia, V., and Quacci, D. Osteoblast-osteocyte transformation. A SEM densitometric analysis of endosteal apposition in rabbit femur. *J Anat* **224**, 132, 2014.
77. Buenzli, P.R. Osteocytes as a record of bone formation dynamics: a mathematical model of osteocyte generation in bone matrix. *J Theor Biol* **364**, 418, 2015.

78. Franz-Odenaal, T.A., Hall, B.K., and Witten, P.E. Buried alive: how osteoblasts become osteocytes. *Dev Dyn* **235**, 176, 2006.
79. Holmbeck, K., Bianco, P., Pidoux, I., *et al.* The metalloproteinase MT1-MMP is required for normal development and maintenance of osteocyte processes in bone. *J Cell Sci* **118**, 147, 2005.
80. Shiflett, L.A., Tiede-Lewis, L.M., Xie, Y., Lu, Y., Ray, E.C., and Dallas, S.L. Collagen Dynamics During the Process of Osteocyte Embedding and Mineralization. *Front Cell Dev Biol* **7**, 178, 2019.
81. Taylor, A.F., Saunders, M.M., Shingle, D.L., Cimbala, J.M., Zhou, Z., and Donahue, H.J. Mechanically stimulated osteocytes regulate osteoblastic activity via gap junctions. *Am J Physiol Cell Physiol* **292**, C545, 2007.
82. Palumbo, C., Palazzini, S., and Marotti, G. Morphological study of intercellular junctions during osteocyte differentiation. *Bone* **11**, 401, 1990.
83. Whitson, S.W. Tight junction formation in the osteon. *Clin Orthop Relat Res* **86**, 206, 1972.
84. Plotkin, L.L., and Bruzzaniti, A. Molecular signaling in bone cells: regulation of cell differentiation and survival. *Adv Protein Chem Struct Biol* **116**, 237, 2019.
85. Buo, A.M., and Stains, J.P. Gap junctional regulation of signal transduction in bone cells. *FEBS Lett* **588**, 1315, 2014.
86. Canalis, E. Notch signaling in osteoblasts. *Sci Signal* **1**, pe17, 2008.
87. Shao, J., Zhou, Y., Lin, J., *et al.* Notch expressed by osteocytes plays a critical role in mineralisation. *J Mol Med* **96**, 333, 2018.
88. Zhao, C., Irie, N., Takada, Y., *et al.* Bidirectional ephrinB2-EphB4 signaling controls bone homeostasis. *Cell Metab* **4**, 111, 2006.
89. Matsuo, K. Cross-talk among bone cells. *Curr Opin Nephrol Hypertens* **18**, 292, 2009.
90. Sahar, N.D., Hong, S.-I., and Kohn, D.H. Micro- and nano-structural analyses of damage in bone. *Micron* **36**, 617, 2005.
91. Wang, L., Ye, T., Deng, L., *et al.* Repair of microdamage in osteonal cortical bone adjacent to bone screw. *PLoS One* **9**, e89343, 2014.
92. Burr, D. Microdamage and bone strength. *Osteoporos Int* **14**, 67, 2003.
93. Burr, D.B. Repair mechanisms for microdamage in bone. *J Bone Miner Res* **29**, 2534, 2014.
94. Hazenberg, J.G., Hentunen, T.A., Heino, T.J., Kurata, K., Lee, T.C., and Taylor, D. Microdamage detection and repair in bone: fracture mechanics, histology, cell biology. *Technol Health Care* **17**, 67, 2009.
95. Wang, R., and Gupta, H.S. Deformation and fracture mechanisms of bone and nacre. *Annu Rev Mater Res* **41**, 41, 2011.
96. Herman, B.C., Cardoso, L., Majeska, R.J., Jepsen, K.J., and Schaffler, M.B. Activation of bone remodeling after fatigue: differential response to linear microcracks and diffuse damage. *Bone* **47**, 766, 2010.
97. Seref-Ferlengez, Z., Basta-Pljakic, J., Kennedy, O.D., Philemon, C.J., and Schaffler, M.B. Structural and mechanical repair of diffuse damage in cortical bone in vivo. *J Bone Miner Res* **29**, 2537, 2014.
98. Head, A. XCVIII. The growth of fatigue cracks. *London Edinburgh Philos Mag J Sci* **44**, 925, 1953.
99. McCreadie, B.R., Hollister, S.J., Schaffler, M.B., and Goldstein, S.A. Osteocyte lacuna size and shape in women with and without osteoporotic fracture. *J Biomech* **37**, 563, 2004.
100. Hazenberg, J.G., Freeley, M., Foran, E., Lee, T.C., and Taylor, D. Microdamage: a cell transducing mechanism based on ruptured osteocyte processes. *J Biomech* **39**, 2096, 2006.
101. Cardoso, L., Herman, B.C., Verborgt, O., Laudier, D., Majeska, R.J., and Schaffler, M.B. Osteocyte apoptosis controls activation of intracortical resorption in response to bone fatigue. *J Bone Miner Res* **24**, 597, 2009.
102. Kennedy, O.D., Laudier, D.M., Majeska, R.J., Sun, H.B., and Schaffler, M.B. Osteocyte apoptosis is required for production of osteoclastogenic signals following bone fatigue in vivo. *Bone* **64**, 132, 2014.
103. Waldorff, E.I., Christenson, K.B., Cooney, L.A., and Goldstein, S.A. Microdamage repair and remodeling requires mechanical loading. *J Bone Miner Res* **25**, 734, 2010.
104. Cen, H.-P., Wu, X.-G., Yu, W.-L., Liu, Q.-Z., and Yia, Y. Effects of the microcrack shape, size and direction on the poroelastic behaviors of a single osteon: a finite element study. *Acta Bioeng Biomech* **18**, 3, 2016.
105. Galley, S.A., Michalek, D.J., and Donahue, S.W. A fatigue microcrack alters fluid velocities in a computational model of interstitial fluid flow in cortical bone. *J Biomech* **39**, 2026, 2006.
106. Wu, X., Wang, Y., Wu, X., Cen, H., Guo, Y., and Chen, W. Effects of microcracks on the poroelastic behaviors of a single osteon. *Sci China Phys Mech* **57**, 2161, 2014.
107. Schaffler, M., Pitchford, W., Choi, K., and Riddle, J. Examination of compact bone microdamage using back-scattered electron microscopy. *Bone* **15**, 483, 1994.
108. Goggin, P., Zygalkakis, K., Oreffo, R., and Schneider, P. High-resolution 3D imaging of osteocytes and computational modelling in mechanobiology: insights on bone development, ageing, health and disease. *Eur Cell Mater* **31**, 264, 2016.
109. Britz, H.M., Thomas, C.D.L., Clement, J.G., and Cooper, D.M. The relation of femoral osteon geometry to age, sex, height and weight. *Bone* **45**, 77, 2009.
110. Currey, J.D. Some effects of ageing in human Haversian systems. *J Anat* **98**, 69, 1964.
111. Jilka, R.L., and O'Brien, C.A. The role of osteocytes in age-related bone loss. *Curr Osteoporos Rep* **14**, 16, 2016.
112. Gabet, Y., and Bab, I. Microarchitectural changes in the aging skeleton. *Curr Osteoporos Rep* **9**, 177, 2011.
113. Frost, H.M. Micropetrosis. *JBSJ* **42**, 144, 1960.
114. Srinivas, V., Bohensky, J., Zahm, A.M., and Shapiro, I.M. Autophagy in mineralizing tissues: microenvironmental perspectives. *Cell Cycle* **8**, 391, 2009.
115. Chen, K., Yang, Y.-H., Jiang, S.-D., and Jiang, L.-S. Decreased activity of osteocyte autophagy with aging may contribute to the bone loss in senile population. *Histochem Cell Biol* **142**, 285, 2014.
116. Bonivitch, A.R., Bonewald, L.F., and Nicoletta, D.P. Tissue strain amplification at the osteocyte lacuna: a microstructural finite element analysis. *J Biomech* **40**, 2199, 2007.
117. Carter, Y., Thomas, C.D.L., Clement, J.G., and Cooper, D.M. Femoral osteocyte lacunar density, volume and morphology in women across the lifespan. *J Struct Biol* **183**, 519, 2013.
118. Hemmatian, H., Bakker, A.D., Klein-Nulend, J., and van Lenthe, G.H. Aging, osteocytes, and mechanotransduction. *Curr Osteoporos Rep* **15**, 401, 2017.

119. Christiansen, P. The skeleton in primary hyperparathyroidism: a review focusing on bone remodeling, structure, mass, and fracture. *APMIS Suppl* **102**, 1, 2001.
120. Kato, Y., Windle, J.J., Koop, B.A., Mundy, G.R., and Bonewald, L.F. Establishment of an osteocyte-like cell line, MLO-Y4. *J Bone Miner Res* **12**, 2014, 1997.
121. Spatz, J.M., Wein, M.N., Gooi, J.H., *et al.* The Wnt inhibitor sclerostin is up-regulated by mechanical unloading in osteocytes in vitro. *J Biol Chem* **290**, 16744, 2015.
122. Kato, Y., Boskey, A., Spevak, L., Dallas, M., Hori, M., and Bonewald, L. Establishment of an osteoid pre-osteocyte-like cell MLO-A5 that spontaneously mineralizes in culture. *J Bone Miner Res* **16**, 1622, 2001.
123. Woo, S.M., Rosser, J., Dusevich, V., Kalajzic, I., and Bonewald, L.F. Cell line IDG-SW3 replicates osteoblast-to-late-osteocyte differentiation in vitro and accelerates bone formation in vivo. *J Bone Miner Res* **26**, 2634, 2011.
124. Wang, K., Le, L., Chun, B.M., *et al.* A novel osteogenic cell line that differentiates into GFP-tagged osteocytes and forms mineral with a bone-like lacunocanalicular structure. *J Bone Miner Res* **34**, 979, 2019.
125. Yang, Y., Wang, M., Yang, S., *et al.* Bioprinting of an osteocyte network for biomimetic mineralization. *Biofabrication* **12**, 045013, 2020.
126. Uchihashi, K., Aoki, S., Matsunobu, A., and Toda, S. Osteoblast migration into type I collagen gel and differentiation to osteocyte-like cells within a self-produced mineralized matrix: a novel system for analyzing differentiation from osteoblast to osteocyte. *Bone* **52**, 102, 2013.
127. Sawa, N., Fujimoto, H., Sawa, Y., and Yamashita, J. Alternating differentiation and dedifferentiation between mature osteoblasts and osteocytes. *Sci Rep* **9**, 1, 2019.
128. Atkins, G.J., Welldon, K.J., Holding, C.A., Haynes, D.R., Howie, D.W., and Findlay, D.M. The induction of a catabolic phenotype in human primary osteoblasts and osteocytes by polyethylene particles. *Biomaterials* **30**, 3672, 2009.
129. Bernhardt, A., Weiser, E., Wolf, S., Vater, C., and Gelinsky, M. Primary human osteocyte networks in pure and modified collagen gels. *Tissue Eng Part A* **25**, 1347, 2019.
130. Takemura, Y., Moriyama, Y., Ayukawa, Y., Kurata, K., Rakhmatia, Y.D., and Koyano, K. Mechanical loading induced osteocyte apoptosis and connexin 43 expression in three-dimensional cell culture and dental implant model. *J Biomed Mater Res A* **107**, 815, 2019.
131. Atkins, G.J., Welldon, K.J., Wijenayaka, A.R., Bonewald, L.F., and Findlay, D.M. Vitamin K promotes mineralization, osteoblast-to-osteocyte transition, and an anticatabolic phenotype by γ -carboxylation-dependent and-independent mechanisms. *Am J Physiol Cell Physiol* **297**, C1358, 2009.
132. Mc Garrigle, M., Mullen, C.A., Haugh, M.G., Voisin, M.C., and McNamara, L.M. Osteocyte differentiation and the formation of an interconnected cellular network in vitro. *Eur Cell Mater* **31**, 323, 2016.
133. Mullen, C.A., Haugh, M.G., Schaffler, M., Majeska, R., and McNamara, L.M. Osteocyte differentiation is regulated by extracellular matrix stiffness and intercellular separation. *J Mech Behav Biomed Mater* **28**, 183, 2013.
134. Kurata, K., Heino, T.J., Higaki, H., and Väänänen, H.K. Bone marrow cell differentiation induced by mechanically damaged osteocytes in 3D gel-embedded culture. *J Bone Miner Res* **21**, 616, 2006.
135. Boukhechba, F., Balaguer, T., Michiels, J.F., *et al.* Human primary osteocyte differentiation in a 3D culture system. *J Bone Miner Res* **24**, 1927, 2009.
136. Sun, Q., Choudhary, S., Mannion, C., Kissin, Y., Zilberberg, J., and Lee, W.Y. Ex vivo construction of human primary 3D-networked osteocytes. *Bone* **105**, 245, 2017.
137. Sun, Q., Choudhary, S., Mannion, C., Kissin, Y., Zilberberg, J., and Lee, W.Y. Ex vivo replication of phenotypic functions of osteocytes through biomimetic 3D bone tissue construction. *Bone* **106**, 148, 2018.
138. Choudhary, S., Sun, Q., Mannion, C., Kissin, Y., Zilberberg, J., and Lee, W.Y. Hypoxic three-dimensional cellular network construction replicates ex vivo the phenotype of primary human osteocytes. *Tissue Eng Part A* **24**, 458, 2018.
139. Gu, Y., Zhang, W., Sun, Q., Hao, Y., Zilberberg, J., and Lee, W.Y. Microbead-guided reconstruction of the 3D osteocyte network during microfluidic perfusion culture. *J Mater Chem B* **3**, 3625, 2015.
140. Guo, X.E., Takai, E., Jiang, X., *et al.* Intracellular calcium waves in bone cell networks under single cell nano-indentation. *Mol Cell Biomech* **3**, 95, 2006.
141. Ma, C., Chang, B., Jing, Y., Kim, H., and Liu, X. Bio-inspired micropatterned platforms recapitulate 3D physiological morphologies of bone and dentinal cells. *Adv Sci* **5**, 1801037, 2018.
142. Chang, B., Ma, C., and Liu, X. Nanofibers Regulate Single Bone Marrow Stem Cell Osteogenesis via FAK/RhoA/YAP1 Pathway. *ACS Appl Mater Interfaces* **10**, 33022, 2018.
143. Smith, L.A., Liu, X., Hu, J., and Ma, P.X. The enhancement of human embryonic stem cell osteogenic differentiation with nano-fibrous scaffolding. *Biomaterials* **31**, 5526, 2010.
144. Matsugaki, A., Matsuzaka, T., Murakami, A., Wang, P., and Nakano, T. 3D printing of anisotropic bone-mimetic structure with controlled fluid flow stimuli for osteocytes: flow orientation determines the elongation of dendrites. *Int J Bioprint* **6**, 106, 2020.
145. Chen, X., Fu, X., Shi, J.-g., and Wang, H. Regulation of the osteogenesis of pre-osteoblasts by spatial arrangement of electrospun nanofibers in two- and three-dimensional environments. *Nanomedicine* **9**, 1283, 2013.
146. You, R., Li, X., Luo, Z., Qu, J., and Li, M. Directional cell elongation through filopodia-steered lamellipodial extension on patterned silk fibroin films. *Biointerphases* **10**, 011005, 2015.
147. Ma, J., He, X., and Jabbari, E. Osteogenic differentiation of marrow stromal cells on random and aligned electrospun poly (L-lactide) nanofibers. *Ann Biomed Eng* **39**, 14, 2011.
148. Prideaux, M., Loveridge, N., Pitsillides, A.A., and Farquharson, C. Extracellular matrix mineralization promotes E11/gp38 glycoprotein expression and drives osteocytic differentiation. *PLoS One* **7**, e36786, 2012.
149. Zhang, Q., Matsui, H., Horiuchi, H., Liang, X., and Sasaki, K. A-Raf and C-Raf differentially regulate mechanobiological response of osteoblasts to guide mechanical stress-induced differentiation. *Biochem Biophys Res Commun* **476**, 438, 2016.
150. Nasello, G., Alamán-Díez, P., Schiavi, J., Pérez, M.Á., McNamara, L., and García-Aznar, J.M. Primary human osteoblasts cultured in a 3D microenvironment create a unique representative model of their differentiation into osteocytes. *Front Bioeng Biotechnol* **8**, 336, 2020.

151. Hirao, M., Hashimoto, J., Yamasaki, N., *et al.* Oxygen tension is an important mediator of the transformation of osteoblasts to osteocytes. *J Bone Miner Metab* **25**, 266, 2007.
152. Gross, T.S., Akeno, N., Clemens, T.L., *et al.* Selected contribution: osteocytes upregulate HIF-1 α in response to acute disuse and oxygen deprivation. *J Appl Physiol* **90**, 2514, 2001.
153. Welldon, K.J., Findlay, D.M., Evdokiou, A., Ormsby, R.T., and Atkins, G.J. Calcium induces pro-anabolic effects on human primary osteoblasts associated with acquisition of mature osteocyte markers. *Mol Cell Endocrinol* **376**, 85, 2013.
154. Atkins, G., Welldon, K., Halbout, P., and Findlay, D. Strontium ranelate treatment of human primary osteoblasts promotes an osteocyte-like phenotype while eliciting an osteoprotegerin response. *Osteoporos Int* **20**, 653, 2009.
155. Kato, H., Ochiai-Shino, H., Onodera, S., Saito, A., Shibahara, T., and Azuma, T. Promoting effect of 1, 25 (OH) 2 vitamin D3 in osteogenic differentiation from induced pluripotent stem cells to osteocyte-like cells. *Open Biol* **5**, 140201, 2015.
156. Prideaux, M., Dallas, S.L., Zhao, N., *et al.* Parathyroid hormone induces bone cell motility and loss of mature osteocyte phenotype through L-calcium channel dependent and independent mechanisms. *PLoS One* **10**, e0125731, 2015.
157. Piard, C., Baker, H., Kamalidinov, T., and Fisher, J. Bioprinted osteon-like scaffolds enhance in vivo neovascularization. *Biofabrication* **11**, 025013, 2019.
158. Andric, T., Sampson, A., and Freeman, J. Fabrication and characterization of electrospun osteon mimicking scaffolds for bone tissue engineering. *Mater Sci Eng C* **31**, 2, 2011.
159. Hejazi, F., and Mirzadeh, H. Roll-designed 3D nanofibrous scaffold suitable for the regeneration of load bearing bone defects. *Prog Biomater* **5**, 199, 2016.
160. Barati, D., Karaman, O., Moeinzadeh, S., Kader, S., and Jabbari, E. Material and regenerative properties of an osteon-mimetic cortical bone-like scaffold. *Regen Biomater* **6**, 89, 2019.
161. Du, Y., Ghodousi, M., Qi, H., Haas, N., Xiao, W., and Khademhosseini, A. Sequential assembly of cell-laden hydrogel constructs to engineer vascular-like microchannels. *Biotechnol Bioeng* **108**, 1693, 2011.
162. Zuo, Y., Xiao, W., Chen, X., Tang, Y., Luo, H., and Fan, H. Bottom-up approach to build osteon-like structure by cell-laden photocrosslinkable hydrogel. *Chem Commun* **48**, 3170, 2012.
163. Zuo, Y., Liu, X., Wei, D., *et al.* Photo-cross-linkable methacrylated gelatin and hydroxyapatite hybrid hydrogel for modularly engineering biomimetic osteon. *ACS Appl Mater Interfaces* **7**, 10386, 2015.
164. Sun, J., Wei, D., Zhu, Y., *et al.* A spatial patternable macroporous hydrogel with cell-affinity domains to enhance cell spreading and differentiation. *Biomaterials* **35**, 4759, 2014.
165. Sun, J., Wei, D., Yang, K., *et al.* The development of cell-initiated degradable hydrogel based on methacrylated alginate applicable to multiple microfabrication technologies. *J Mater Chem B* **5**, 8060, 2017.
166. Li, M., Fu, X., Gao, H., Ji, Y., Li, J., and Wang, Y. Regulation of an osteon-like concentric microgrooved surface on osteogenesis and osteoclastogenesis. *Biomaterials* **216**, 119269, 2019.
167. Despang, F., Bernhardt, A., Lode, A., *et al.* Synthesis and physicochemical, in vitro and in vivo evaluation of an anisotropic, nanocrystalline hydroxyapatite bisque scaffold with parallel-aligned pores mimicking the microstructure of cortical bone. *J Tissue Eng Regen Med* **9**, E152, 2015.
168. Chen, X., Ergun, A., Gevgilili, H., Ozkan, S., Kalyon, D.M., and Wang, H. Shell-core bi-layered scaffolds for engineering of vascularized osteon-like structures. *Biomaterials* **34**, 8203, 2013.
169. Wei, D., Sun, J., Bolderson, J., *et al.* Continuous fabrication and assembly of spatial cell-laden fibers for a tissue-like construct via a photolithographic-based microfluidic chip. *ACS Appl Mater Interfaces* **9**, 14606, 2017.
170. Zhang, M., Lin, R., Wang, X., *et al.* 3D printing of Haversian bone-mimicking scaffolds for multicellular delivery in bone regeneration. *Sci Adv* **6**, eaaz6725, 2020.

Address correspondence to:

Xiaohua Liu, PhD
Department of Biomedical Sciences
Texas A&M University College of Dentistry
3302 Gaston Avenue
Dallas, TX 75246
USA

E-mail: xliu1@tamu.edu

Received: October 23, 2020

Accepted: January 22, 2021

Online Publication Date: March 8, 2021